Good practice guide for checking the measurement performance of five axes milling machine tools

Bojan Ačko

University of Maribor (UM)
Maribor, Slovenia

Lisa Groos, Christian Held, Frank Keller, Klaus Wendt

Physikalisch-Technische Bundesanstalt (PTB)
Braunschweig, Germany

Hichem Nouira, Fabien Viprey

Laboratoire national de métrologie et d'essais (LNE)
Paris, France

We gratefully acknowledge the funding from the European Metrology Research Programme (EMRP). The EMRP is jointly funded by the EMRP participating countries within EURAMET and the European Union.

Table of Contents

List of Figures

1 Introduction

A typical machine tool (MT) has three perpendicular linear axes, and often one or two additional rotation axes. Movements of these axes allow changing the relative position and orientation between the tool and the workpiece. Systematic deviations between the nominal value and the real value of the relative position and orientation are called geometric errors. Such geometric errors of the machine tool lead to systematic manufacturing or measurement errors. In order to increase the manufacturing and measurement accuracy it is hence necessary to measure and correct these errors. Nowadays the correction can be performed by software tools implemented in the machine tool controller, which makes the correction much easier, cheaper and more flexible than a mechanical correction of the guideways.

In order to measure and correct the geometric errors, a kinematic model of the machine tool is used. In principle the geometric errors could be measured directly for a number of sufficiently dense grid points in the working volume. However, this soon leads to a number of more than 10000 points which have to be measured. Using a suitable model of the machine tool reduces the measurement expense significantly. In Section 2 the error model according to the ISO standard 230-1 [1] is briefly described, while in Section 3 and Section 4 strategies for the measurement of these errors are presented.

When measuring the geometric errors of a machine tool, one normally cannot ensure that the environmental temperature has a defined value. Therefore it is necessary, that the temperature influence on the measuring instruments or artefacts used for the measurement is negligible or can be compensated. For the measurements with a laser interferometer as presented in Section 3 this is achieved by monitoring environmental parameters (temperature, humidity, air pressure) and accordingly apply corrections to the measurement. When using artefacts as described in Section 4 (and also Section 5), it is necessary that these artefacts have a thermal expansion coefficient of almost zero.

Even if the geometric errors of a machine tool are compensated, there still exist residual errors, i.e. errors which remain after the correction, e.g. due to non-model-conform behaviour of the machine tool. In order to assess the measurement accuracy of a machine tool these residual errors must be taken into account. In Section 5 a fast method to verify the accuracy with the help of ball bars is given.

2 Volumetric error model

Many different volumetric error models for machine tools have been discussed in the literature. However, it is advised to follow the ISO standard 230-1 [1], since measurement software tools and correction algorithms for MT controllers normally support these methods. This section should give a brief survey about the concept.

2.1 Error model for linear axes

According to ISO 230-1 the errors of the linear axes are modelled as three concatenated rigid bodies. We hence have 3×6 parameters to describe the movement of the three bodies, where the parameters are functions of the nominal value of the according axis. For each axis, this is a position error in the direction of the axis, two straightness errors perpendicular to the axis, and further three orientation errors describing the orientation deviation of the carriage which moves along the axis. Additionally there are three squareness errors, which describe deviations of the perpendicularity between the three axes. Note that squareness errors can also be included as a linear term into straightness errors, or as a constant term into rotational errors.

To be more precise, for the kinematic chain of t-Y-X-Z-w from tool to workpiece, as it may typically occur for a machine tool with horizontal working spindle, the coordinates of the tool tip are calculated by

$$p(x,y,z) = R_Z(z)\big[R_X(x)\big(R_Y(y)T + ye_Y + b_Y(y)\big) + xe_X + b_X(x)\big] + ze_Z + b_Z(z),$$

for nominal axis position (x,y,z). Here T is the vector describing the tool offset (probe offset or reflector offset when checking the measurement performance), and $R_X(x), b_X(x)$ are rotational and linear displacement errors for the *x*-axis (respectively for the other axes). To be more precise, the linear displacement errors are given by

$$b_X(x) = \begin{pmatrix} E_{XX}(x) \\ E_{YX}(x) \\ E_{ZX}(x) \end{pmatrix} + \begin{pmatrix} 0 \\ 0 \\ -E_{BOX} \cdot x \end{pmatrix}$$

$$b_Y(y) = \begin{pmatrix} E_{XY}(y) \\ E_{YY}(y) \\ E_{ZY}(y) \end{pmatrix} + \begin{pmatrix} -E_{COY} \cdot y \\ 0 \\ E_{AOY} \cdot y \end{pmatrix}$$

and

$$b_Z(z) = \begin{pmatrix} E_{XZ}(z) \\ E_{YZ}(z) \\ E_{ZZ}(z) \end{pmatrix}.$$

The rotational errors for each axis are described by the matrices $R_X, R_Y, R_Z \in SO(3)$, which are rotations close to the identity. There hence exits skew-symmetric matrices $H_X, H_Y, H_Z \in so(3)$ near to zero such that

$$R_X = e^{H_X} = \mathbb{E}_{3\times3} + H_X + \frac{1}{2}H_X^2 + \cdots,$$

and analogous for the other axes. Here, $\mathbb{E}_{3\times3}$ denotes the 3×3-identity matrix. The components for $H_X(x)$ are given by the rotational errors for the *x*-axis, i.e.

$$H_X(x) = \begin{pmatrix} 0 & -E_{CX}(x) & E_{BX}(x) \\ E_{CX}(x) & 0 & -E_{AX}(x) \\ -E_{BX}(x) & E_{AX}(x) & 0 \end{pmatrix},$$

and for the *y*- and *z*-axis respectively. For small rotational errors, the rotation R_X can therefore be linearly approximated by

$$R_X \approx \mathbb{E}_{3\times3} + H_X = \begin{pmatrix} 1 & -E_{CX} & E_{BX} \\ E_{CX} & 1 & -E_{AX} \\ -E_{BX} & E_{AX} & 1 \end{pmatrix}.$$

The geometric error vector at the tool tip position for nominal axis position (x,y,z) is the difference between the real position and the nominal position of the tool tip, i.e.

$$e(x,y,z) = p(x,y,z) - p_{nom}(x,y,z)$$

with $p_{nom}(x,y,z) = T + xe_x + ye_y + ze_z$ the nominal coordinates of the tool tip.

Since the geometric error vector is not a linear function of all parametric errors, a linearization is performed as follows.

$$
\begin{aligned}
e(x,y,z) = \;& p(x,y,z) - p_{nom}(x,y,z) \\
= \;& R_Z(z)\big[R_X(x)\big(R_Y(y)T + ye_Y + b_Y(y)\big) + xe_X + b_X(x)\big] + ze_Z + b_Z(z) - T - xe_x - ye_y - ze_z \\
= \;& (R_Z(z)R_X(x)R_Y(y) - \mathbb{E}_{3\times3})T + (R_Z(z)R_X(x) - \mathbb{E}_{3\times3})ye_Y + R_Z(z)R_X(x)b_Y(y) \\
& + (R_Z(z) - \mathbb{E}_{3\times3})xe_x + R_Z(z)b_X(x) + b_Z(z) \\
\approx \;& \big(H_Z(z) + H_X(x) + H_Y(y)\big)T + (H_Z(z) + H_X(x))ye_Y + R_Z(z)R_X(x)b_Y(y) + H_Z(z)xe_x \\
& + R_Z(z)b_X(x) + b_Z(z) \\
\approx \;& \big(H_Z(z) + H_X(x) + H_Y(y)\big)T + (H_Z(z) + H_X(x))ye_Y + b_Y(y) + H_Z(z)xe_x + b_X(x) + b_Z(z)
\end{aligned}
$$

For the approximation it was made use of formulas like

$$R_X R_Y \approx (\mathbb{E}_{3\times3} + H_X)(\mathbb{E}_{3\times3} + H_Y) \approx (\mathbb{E}_{3\times3} + H_X + H_Y)$$

and

$$R_X b_Y \approx (\mathbb{E}_{3\times3} + H_X)b_Y \approx b_Y$$

for small H_X, H_Y, and relatively small b_Y compared to the size of the working volume. Note further that

$$\begin{pmatrix} 0 & -c & b \\ c & 0 & -a \\ -b & a & 0 \end{pmatrix}\begin{pmatrix} x \\ y \\ z \end{pmatrix} = \begin{pmatrix} a \\ b \\ c \end{pmatrix} \times \begin{pmatrix} x \\ y \\ z \end{pmatrix} = \begin{pmatrix} 0 & z & -y \\ -z & 0 & x \\ y & -x & 0 \end{pmatrix}\begin{pmatrix} a \\ b \\ c \end{pmatrix}$$

for all $a, b, c, x, y, z \in \mathbb{R}$. Using this, it follows with $T = (t_X, t_Y, t_Z)^t$ that

$$
\begin{aligned}
e(x,y,z) = \;& \begin{pmatrix} 0 & t_Z & -t_Y \\ -t_Z & 0 & t_X \\ t_Y & -t_X & 0 \end{pmatrix}\begin{pmatrix} E_{AX} + E_{AY} + E_{AZ} \\ E_{BX} + E_{BY} + E_{BZ} \\ E_{CX} + E_{CY} + E_{CZ} \end{pmatrix} + \begin{pmatrix} 0 & 0 & -y \\ 0 & 0 & 0 \\ y & 0 & 0 \end{pmatrix}\begin{pmatrix} E_{AX} + E_{AZ} \\ E_{BX} + E_{BZ} \\ E_{CX} + E_{CZ} \end{pmatrix} \\
& + \begin{pmatrix} E_{XY} \\ E_{YY} \\ E_{ZY} \end{pmatrix} + \begin{pmatrix} -E_{COY} \cdot y \\ 0 \\ E_{AOY} \cdot y \end{pmatrix} + \begin{pmatrix} 0 & 0 & 0 \\ 0 & 0 & x \\ 0 & -x & 0 \end{pmatrix}\begin{pmatrix} E_{AZ} \\ E_{BZ} \\ E_{CZ} \end{pmatrix} + \begin{pmatrix} E_{XX} \\ E_{YX} \\ E_{ZX} \end{pmatrix} + \begin{pmatrix} 0 \\ 0 \\ -E_{BOX} \cdot x \end{pmatrix} + \begin{pmatrix} E_{XZ} \\ E_{YZ} \\ E_{ZZ} \end{pmatrix} \\
= \;& \begin{pmatrix} E_{XX} \\ E_{YX} \\ E_{ZX} \end{pmatrix} + \begin{pmatrix} E_{XY} \\ E_{YY} \\ E_{ZY} \end{pmatrix} + \begin{pmatrix} E_{XZ} \\ E_{YZ} \\ E_{ZZ} \end{pmatrix} + \begin{pmatrix} 0 & t_Z & -t_Y - y \\ -t_Z & 0 & t_X \\ t_Y + y & -t_X & 0 \end{pmatrix}\begin{pmatrix} E_{AX} \\ E_{BX} \\ E_{CX} \end{pmatrix} + \begin{pmatrix} 0 & t_Z & -t_Y \\ -t_Z & 0 & t_X \\ t_Y & -t_X & 0 \end{pmatrix}\begin{pmatrix} E_{AY} \\ E_{BY} \\ E_{CY} \end{pmatrix} \\
& + \begin{pmatrix} 0 & t_Z & -t_Y - y \\ -t_Z & 0 & t_X + x \\ t_Y + y & -t_X - x & 0 \end{pmatrix}\begin{pmatrix} E_{AZ} \\ E_{BZ} \\ E_{CZ} \end{pmatrix} + \begin{pmatrix} 0 & 0 & -y \\ 0 & 0 & 0 \\ -x & y & 0 \end{pmatrix}\begin{pmatrix} E_{BOX} \\ E_{AOY} \\ E_{COY} \end{pmatrix}
\end{aligned}
$$

From this form it can easily be seen how to construct a model matrix $C \in M(3 \times 21)$ depending on the coordinates x, y, z and the tool lengths t_X, t_Y, t_Z, such that $e(x,y,z) = C \cdot \phi$, where

$$\phi = (E_{XX}, E_{YX}, E_{ZX}, E_{AX}, E_{BX}, E_{CX}, E_{XY}, \dots, E_{XZ}, \dots, E_{BZ}, E_{CZ}, E_{BOX}, E_{AOY}, E_{COY})^t$$

is a vector containing all 21 parametric errors at the coordinates x, y, z. More precisely, with the definitions

$$C_X = \begin{pmatrix} 1 & 0 & 0 & 0 & t_Z & -t_Y - y \\ 0 & 1 & 0 & -t_Z & 0 & t_X \\ 0 & 0 & 1 & t_Y + y & -t_X & 0 \end{pmatrix} \qquad C_Y = \begin{pmatrix} 1 & 0 & 0 & 0 & t_Z & -t_Y \\ 0 & 1 & 0 & -t_Z & 0 & t_X \\ 0 & 0 & 1 & t_Y & -t_X & 0 \end{pmatrix}$$

$$C_Z = \begin{pmatrix} 1 & 0 & 0 & 0 & t_Z & -t_Y - y \\ 0 & 1 & 0 & -t_Z & 0 & t_X + x \\ 0 & 0 & 1 & t_Y + y & -t_X - x & 0 \end{pmatrix} \qquad C_W = \begin{pmatrix} 0 & 0 & -y \\ 0 & 0 & 0 \\ -x & y & 0 \end{pmatrix}$$

one has $C = (C_X, C_Y, C_Z, C_W)$.

2.2 Rotary axes

Each rotary axis is modelled as a rigid body and has therefore six component errors, which are functions of the rotation angle. Furthermore, each axis has two position and two orientation errors. Note that the component and position/orientation errors depend on each other.

Suppose that the nominal centre of rotation is the origin. The nominal position of a point x rotated around the nominal axis $n \in \mathbb{R}^3$ (with$|n| = 1$) by the angle α is then given by

$$p_{nom}(\alpha, x) = R(\alpha)x.$$

with

$$R(\alpha) = e^{\alpha \cdot \hat{n}} = \mathbb{E}_{3\times 3} + \sin\alpha \cdot \hat{n} + (1 - \cos\alpha) \cdot \hat{n}^2$$

Here $\hat{n} \in so(3)$ denotes the matrix

$$\hat{n} = \begin{pmatrix} 0 & -n_3 & n_2 \\ n_3 & 0 & -n_1 \\ -n_2 & n_1 & 0 \end{pmatrix}$$

for $n = (n_1, n_2, n_3)^t$.

Let now $B(\alpha)$ be the component rotational error and $b(\alpha)$ the component position errors. Moreover, let the actual rotational axis be given by $n' = S \cdot n$, where S is a (small) rotation. Since $\widehat{n'} = S\hat{n}S^{-1}$, a rotation around n' by the angle α is the given by $SR(\alpha)S^{-1}$. Moreover, let $d \in \mathbb{R}^3$ be the position error of the rotational axis, measured orthogonal to the nominal axis. Then the real position, subjected to geometric errors, of a point x rotated by the angle α is given by

$$p(\alpha, x) = B(\alpha) \cdot S \cdot R(\alpha) \cdot S^{-1}(x - d) + d + b(\alpha)$$

Using the linear approximations $S \approx \mathbb{E}_{3\times 3} + K$ and $B(\alpha) \approx \mathbb{E}_{3\times 3} + H(\alpha)$ with $K, B(\alpha) \in so(3)$ for small rotations, this can be written as

$$\begin{aligned} p(\alpha, x) &\approx \big(1 + H(\alpha)\big) \cdot (1 + K) \cdot R(\alpha) \cdot (1 - K) \cdot (x - d) + b(\alpha) + d \\ &= (1 + H(\alpha) + K) \cdot R(\alpha) \cdot (1 - K) \cdot (x - d) + b(\alpha) + d \\ &= (\, R(\alpha) + H(\alpha)R(\alpha) + SR(\alpha) - R(\alpha)S\,) \cdot (x - d) + b(\alpha) + d \end{aligned}$$

The error vector at $p_{nom}(\alpha, x)$ is then given by

$$e(\alpha, x) = p(\alpha, x) - p_{nom}(\alpha, x).$$

With a similar approach as for the linear axis it is now possible to write the error vector as a linear function of the parametric errors. Unfortunately one cannot assume the position error d to be small, since d is dependent from the choice of coordinate system. Recall that the origin of the calculated coordinate system depends on the specified reflector offset, which can have an uncertainty of several millimetres. However, it is possible to iteratively calculate and correct the position error d during the multi-lateration. Note, however, that the final result for the position error d is useless due to the unknown precise origin of the coordinate system.

3 Volumetric error mapping via sequential multi-lateration (PTB)

For the measurement of the geometric errors exist different methods. Most methods use material standards like hole plates or ball plates. In Section 4 the usage of a newly developed hole bar is described. In this section the measurements using a tracking laser interferometer is described.

3.1 Determination of parametric errors of linear axes by sequential multi-lateration

Under the assumption of the just described rigid body model according to ISO 230-1, the parametric errors can be determined by a series of length measurements with a tracking interferometer and sequential multi-lateration [4],[5]. To this aim, the tracking interferometer is placed at different positions in (or near) the working volume. One needs at least four non-coplaner positions. For each position the lengths between a fixed reference ball of the laser interferometer and a reflector are measured for a number of grid points in the working volume. The reflector is mounted in or near the working spindle. The position of the reflector must not be the same for all interferometer positions, but one needs at least three non-colinear positions in order to determine all rotational errors. The vector from a reference point on the spindle axis to the reflector is the reflector offset. The reference point can be chosen arbitrarily, but for the correction of the MT the same reference point must be used to measure the tool offset.

The positions of the interferometer must be known only roughly and can later be calculated exactly from the measurement data. Also, the length measurements of the interferometer are subjected to one or more unknown dead path lengths per interferometer position, since only length changes to an estimated initial length can be measured. These dead path lengths are also calculated exactly from the measurement results. The reflector offsets must be measured before the measurement. However, it is sufficient to know the offset with a precision of one or two millimetre, since the effect of a length change in this range to the geometric error is very small.

In the following, the mathematical background of the sequential multi-lateration for the parametric error detection should be briefly discussed. Denote the initial (only roughly known) positions of the interferometer by $q_1, q_2, \dots, q_r$. For each position i the reflector moves to the nominal positions $p_{i1}, p_{i2}, \dots, p_{in_i}$ in the working volume. The nominal distances between reflector and (reference ball) of the laser interferometer are thus

$$(l_{nom})_{ij} = |p_{ij} - q_i|$$

for $i = 1, \dots, r$ and $j = 1, \dots, m_r$. Since the positions of the interferometer are not known exactly, we introduce vectors $t_1, \dots, t_r$ such that $q_i - t_i$ are the unknown real positions. Moreover, the nominal positions of the reflector have to be corrected by the volumetric errors e_{ij}, so $p_{ij} + e_{ij}$ are the real positions. The real distances are hence

$$l_{ij} = |p_{ij} + e_{ij} - q_i + t_i|.$$

The measured distances of the laser interferometer $(l_m)_{ij}$ have to be corrected by unknown dead path lengths $l_{0,i}$, i.e. $l_{ij} = (l_m)_{ij} + l_{0,i}$. Finally the differences between the real lengths and nominal lengths are given by

$$l_{ij} - (l_{nom})_{ij} = |p_{ij} - q_i + e_{ij} + t_i| - |p_{ij} - q_i|.$$

If we write $v_{ij} = p_{ij} - q_i$ and $u_{ij} = e_{ij} + t_i$, we have

$$\begin{aligned}(l_{nom})_{ij} = &\ \sqrt{\langle v_{ij} + u_{ij}, v_{ij} + u_{ij}\rangle} - \sqrt{\langle v_{ij}, v_{ij}\rangle} \\ = &\ |v_{ij}|\left(\sqrt{1 + 2\left\langle \frac{v_{ij}}{|v_{ij}|}, \frac{u_{ij}}{|v_{ij}|}\right\rangle + \left\langle \frac{u_{ij}}{|v_{ij}|}, \frac{u_{ij}}{|v_{ij}|}\right\rangle} - 1\right)\end{aligned}$$

$$= \quad |v_{ij}|\left(1+\frac{1}{2}\left(2\,\langle\frac{v_{ij}}{|v_{ij}|},\frac{u_{ij}}{|v_{ij}|}\rangle+\ \langle\frac{u_{ij}}{|v_{ij}|},\frac{u_{ij}}{|v_{ij}|}\rangle\right)+\cdots-1\right)$$

$$= \quad \langle\frac{v_{ij}}{|v_{ij}|},u_{ij}\rangle+\cdots$$

Here, the series expansion $\sqrt{1+x}=1+\frac{1}{2}x-\frac{1}{8}x^2+\cdots$ for $|x|\leq 1$ was used, and $\langle\cdot,\cdot\rangle$ denotes the usual scalar (or dot) product in $\mathbb{R}^3$. In first order approximation in $\frac{u_{ij}}{|v_{ij}|}=\frac{e_{ij}+t_i}{|p_{ij}-q_i|}$ it thus follows that

$$(l_m)_{ij}-(l_{nom})_{ij}=\langle n_{ij},e_{ij}+t_i\rangle-l_{0,i}=n_{ij}^t(e_{ij}+t_i)-l_{0,i}$$

with $n_{ij}=\frac{p_{ij}-q_i}{|p_{ij}-q_i|}$. In other words, the difference of the nominal lengths and the measured lengths plus the dead path lengths are approximately given by the projection of the error e_{ij} and the deviation of the interferometer position t_i onto the nominal measurement line n_{ij}, see Figure 1

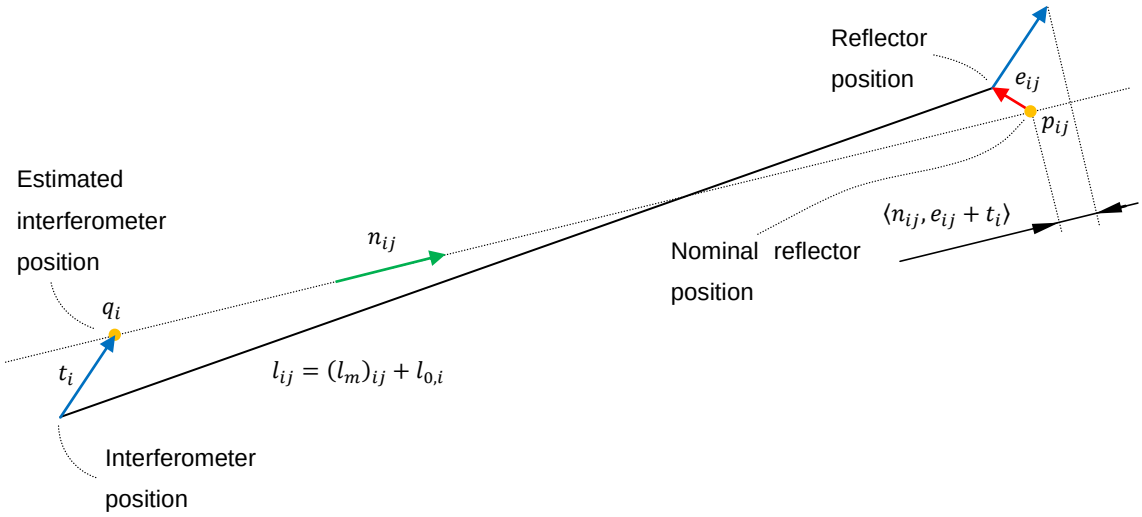

Figure 1: Geometric error and interferometer displacement projected onto the nominal measurement line

Recall that in first order approximation the geometric errors e_{ij} depend linearly on the parametric errors for this grid point. Therefore we can write $e_{ij}=C(p_{ij})\phi(p_{ij})$, where $C_{ij}=C(p_{ij})\in M(3\times 21)$ is the matrix describing the error model for the point p_{ij}, and $\phi_{ij}=\phi(p_{ij})$ are the 21 parametric errors for the points p_{ij}. We can write the above equation into a single matrix equation for the point p_{ij} and interferometer position q_i:

$$(l_m)_{ij}-(l_{nom})_{ij}=\left(n_{ij}^t(C_{ij},\mathbb{E}_{3\times 3}),-\mathbb{E}_{3\times 3}\right)\begin{pmatrix}\phi_{ij}\\ t_i\\ l_{0,i}\end{pmatrix}.$$

The next step is now to combine these equations for all measured distances into a single matrix equation. We start with the construction of a matrix $\tilde{C}$ such that $\tilde{C}\tilde{\phi}=e$ with $\tilde{\phi}$ the parametric errors for all grid points (these are $6\cdot(d_1+d_2+d_3)+3$ values) and $e=(e_{ij})$ the geometric errors for all points p_{ij}. To this aim one has to remember that the points p_{ij} lie on a grid of size $d_1\times d_2\times d_3$. Thus there are numbers $x_1,\dots x_\mu,\dots x_{d_1}$, $y_1,\dots,y_\nu,\dots,y_{d_2}$, and $z_1,\dots,z_\tau,\dots,z_{d_3}$, such that each reflector position p_{ij} and the geometric error e_{ij} in this point can be written as

$$p_{ij}=(x_\mu,y_\nu,z_\tau)^t+T_i$$

for appropriate μ, ν, τ. Here T_i denotes the reflector offset for interferometer position i. Similarly we can define

$$\phi_{X,\mu} = \left(E_{XX}(x_\mu), E_{YX}(x_\mu), E_{ZX}(x_\mu), E_{AX}(x_\mu), E_{BX}(x_\mu), E_{CX}(x_\mu)\right)$$

and $\phi_{Y,\nu}$ and $\phi_{Z,\tau}$ accordingly. Then $\tilde{\phi}$ is the vector

$$\tilde{\phi} = \left(\phi_{X,1}, \phi_{X,2}, \dots, \phi_{X,d_1}, \phi_{Y,1}, \phi_{Y,2}, \dots, \phi_{Y,d_2}, \phi_{Z,1}, \phi_{Z,2}, \dots, \phi_{Z,d_3}, E_{BOX}, E_{AOY}, E_{COY}\right)^t.$$

The above defined matrices C_X, C_Y, C_Z become now

$$C_{X,\mu,\nu,\tau}(T) = \begin{pmatrix} 1 & 0 & 0 & 0 & t_Z & -t_Y - y_\nu \\ 0 & 1 & 0 & -t_Z & 0 & t_X \\ 0 & 0 & 1 & t_Y + y_\nu & -t_X & 0 \end{pmatrix},$$

and $C_{Y,\mu,\nu,\tau}(T)$ and $C_{Z,\mu,\nu,\tau}(T)$, respectively. Finally, the geometric error $e_{ij} = e_{\mu\nu\tau}$ is given by

$$\left(0, \dots, 0, C_{X,\mu,\nu,\tau}(T_i), 0, \dots, 0, C_{Y,\mu,\nu,\tau}(T_i), 0, \dots, 0, C_{Z,\mu,\nu,\tau}(T_i), 0, \dots, 0, C_W\right)\tilde{\phi} = e_{ij}$$

with $C_{X,\mu,\nu,\tau}(T_i)$ in the position such that it matches $\phi_{X,\mu}$ in $\tilde{\phi}$, and so on. The matrix $\tilde{C}$ is now the combination of all such rows, and it follows $\tilde{C}\tilde{\phi} = e$ as desired.

Let now K_1 be the matrix which maps the improvements t_i of the interferometer positions to the according positions in the vector $e = (e_{ij})$, i.e. such that

$$\tilde{C}\tilde{\phi} + K_1 \begin{pmatrix} t_1 \\ t_2 \\ \vdots \\ t_r \end{pmatrix} = \begin{pmatrix} e_{11} + t_1 \\ e_{12} + t_1 \\ \vdots \\ e_{21} + t_2 \\ \vdots \\ e_{r,k_r} + t_r \end{pmatrix}$$

For the projections onto the vectors n_{ij} the matrix

$$N = \begin{pmatrix} n_{11}^t & \cdots & 0 \\ \vdots & \ddots & \vdots \\ 0 & \cdots & n_{r,k_r}^t \end{pmatrix}$$

is introduced, so that

$$N \cdot \tilde{C}\tilde{\phi} + \; N \cdot K_1 \begin{pmatrix} t_1 \\ \vdots \\ t_r \end{pmatrix} = N \cdot \left(\tilde{C}, K_1\right) \cdot \begin{pmatrix} \tilde{\phi} \\ t_1 \\ \vdots \\ t_r \end{pmatrix} = \begin{pmatrix} \langle n_{11}, e_{11} + t_1 \rangle \\ \langle n_{12}, e_{12} + t_1 \rangle \\ \vdots \\ \langle n_{21}, e_{21} + t_2 \rangle \\ \vdots \\ \langle n_{r,n_r}, e_{r,k_r} + t_r \rangle \end{pmatrix}$$

It remains to include the dead path lengths $l_{0,i}$, so let K_2 be the matrix which maps the dead path lengths to the corresponding (i,j)-positions, i.e. such that

$$K_2 \begin{pmatrix} l_{0,1} \\ l_{0,2} \\ \vdots \\ l_{0,r} \end{pmatrix} = \left.\begin{pmatrix} l_{0,1} \\ l_{0,1} \\ \vdots \\ l_{0,2} \\ \vdots \\ l_{0,r} \end{pmatrix}\right\} k_1 + k_2 + \dots + k_r \text{ values}$$

(It was supposed here that there is only one dead path length for each interferometer position. However, this easily could be generalized to several dead path lengths per position by adapting the matrix K_2 accordingly.)

Putting all together, one gets with $M = N \cdot \left(\tilde{C}, K_1\right)$ the equation

$$(M, -K_2)\psi = L_m - L_{nom},$$

where ψ includes the parametric errors for all grid points as well as all t_i and $l_{0,i}$, and further L_m all measured lengths, and L_{nom} all nominal lengths (these are $n_1 + n_2 + \cdots n_r$ values).

Finally we imply the following boundary conditions: All parametric errors are set to zero in the first measurement point of the axis, and all straightness errors are additionally set to zero in the last measurement point of the axis. With a suitable matrix B this can be written as $B\tilde{\phi} = 0$. (Each row of B consists of zeros and exactly one 1, which picks the corresponding entry in $\tilde{\phi}$ which is set to zero.)

We finally get the matrix equation

$$\begin{pmatrix} M & -K \\ B & 0 \end{pmatrix} \psi = \begin{pmatrix} \Delta L \\ 0 \end{pmatrix}$$

where $\Delta L = L_m - L_{nom}$. However, the above equation is highly overdetermined and only valid in first order approximation in the values $\frac{u_{ij}}{|v_{ij}|} = \frac{e_{ij}+t_i}{|p_{ij}-q_i|}$. We hence should rather write this as iteration

$$\psi^{(n+1)} = \mathrm{argmin}_{\psi} \left\| \begin{pmatrix} M^{(n)} & -K \\ B & 0 \end{pmatrix} \psi - \begin{pmatrix} \Delta L \\ 0 \end{pmatrix} \right\|_2$$

to find the values for the parametric errors, the remaining correction values for the interferometer position, and the dead path lengths. Note that that the matrix $M^{(n)}$ changes after each iteration since it depends on the tracer positions $q_i^{(n)}$, which have to be corrected by the new values for $t_i^{(n)}$ after each iteration, i.e. $q_i^{(n+1)} = q_i^{(n)} - t_i^{(n)}$. The minimization problem itself is an ordinary linear least square problem, which can be solved e.g. using the QR-decomposition of the matrix on the left hand side.

3.2 Uncertainty estimation

Since the mathematical procedure for the calculation of the volumetric errors out of the measured lengths is somehow complicated, the most suitably way of calculating the uncertainty is by a Monte-Carlo simulation. Therefore a simple uncertainty model for the length measurements is assumed, which consists of a constant and a length dependent part, see [4] for more details. The uncertainty of the reflector offset is also taken into account. By varying the values for the input data according to the model and recalculation of the volumetric errors for 100 repetitions, the uncertainties of the volumetric errors can be estimated by considering the 95%-coverage interval.

3.3 Measurement procedure for linear axes

The measurements of the geometric errors of the linear axes can be performed using a tracking laser interferometer. The geometric errors can then be calculated by the procedure described in Section 3.1. A similar approach for the measurement of the geometric errors of the rotary axis is possible. For the best results, the following points should be considered:

- For small uncertainties of the volumetric errors measured by sequential multi-lateration, the different measurement positions of the laser tracer should have a maximal range in each coordinate direction.
- It is recommended to fix the reflector mechanically near to the working spindle, rather than mounting it directly in the working spindle with an adapted tool holder.
- A direct communication between the measurement software and the machine tool controller could increase the speed of measurement.
- The mounting device for the laser interferometer should be designed such that it allows easy and fast mounting on the working table.

- If the machine tool is equipped with rotary axes, the linear axes should be measured *and* corrected before the measurement of the rotary axes. Otherwise the errors of the linear axes contribute to the errors of the rotary axes.

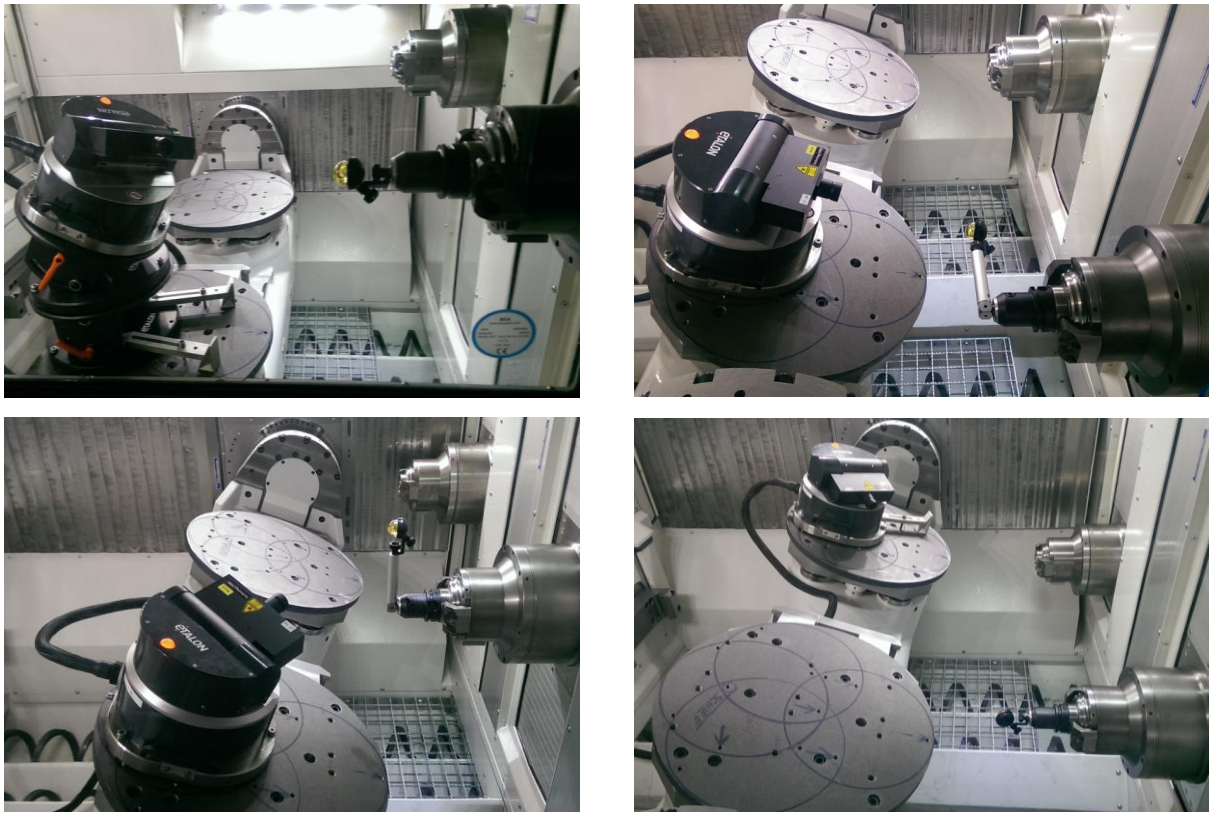

Figure 2: Different positions of interferometer and reflector for geometric error mapping

3.4 Measurement procedure for rotary axes

The measurement of the rotary axis is performed independently of the measurement of the linear axis. However, since the coordinate system for the measurement is defined by the linear axes, it is recommended to measure *and correct* the linear axes before the measurement of the rotary axis.

The measurement principle for the rotary axis is similar to the measurement of the linear axis. The laser interferometer has to be mounted on the rotary table or swivel axis on at least three non-colinear positions. The reflector is mounted in or near to the spindle, and is moved by the linear axis to at least four non-coplanar positions. Possible configurations of the interferometer and reflector for the measurement of swivel axis and rotary table are given in Figure 3. Note that the relative position of the reflector to the reference point on the spindle must not change during the measurement. Length measurements are taken for all tracer and reflector positions at equidistant angular positions of the rotary axis. With a similar mathematical approach as for the linear axis, the geometric errors as well as the tracer positions can be calculated.

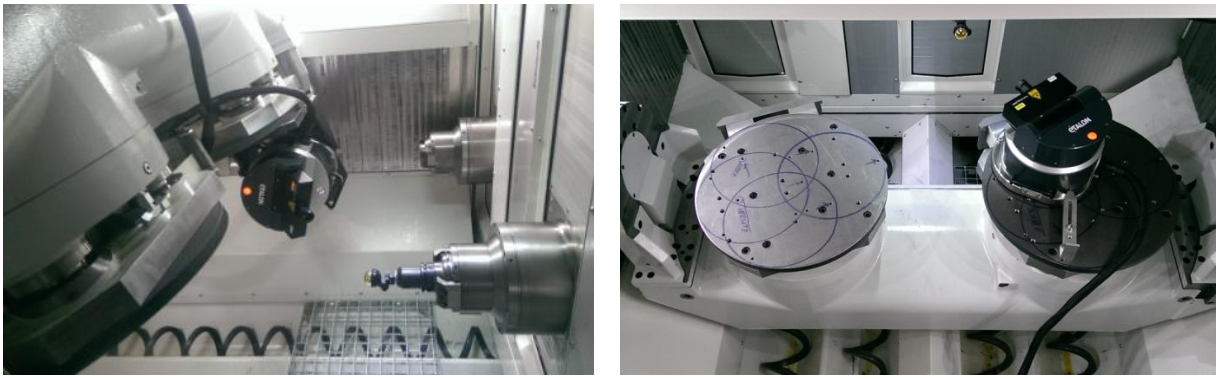

Figure 3: Measurement of the swivel axis and rotary table

3.5 Temperature influence

Since the machine tool geometry is strongly influenced by temperature, the measurement should take place at a constant environmental temperature. It is recommended to track the environmental temperature as well as the machine tool temperate at several locations. Moreover, the machine tool should be warmed up prior to the measurement procedure, such that the machine tool is in similar condition as for the production. To this aim, the machine tool should perform a warm-up cycle for about one hour, where all axis and the spindle are moved.

If the geometric errors of a machine tool should be measured at different environmental temperatures, the machine tool can be housed in a portal climate chamber, see for example [3] for the description of such a climate chamber and its use. Note that the machine tool must be given sufficient time to acclimatize. For a medium sized machine tool this time should be at least 48 hours.

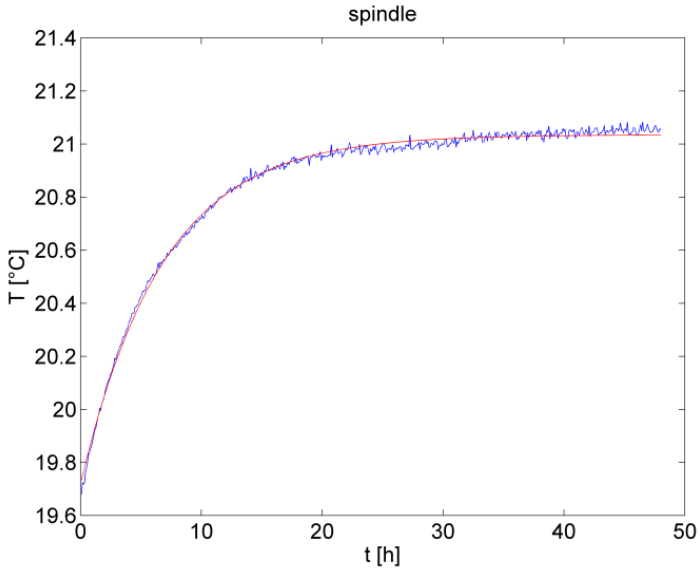

Figure 4: Spindle temperature at a change of the environmental temperature from 20 °C to 25 °C

Figure 4 shows the spindle temperature in dependence of the time for a temperature change of the environmental temperature from 20 °C to 25 °C for an investigated machine tool. The final temperature the spindle reaches is about 21 °C. This temperature is lower than the environmental temperature since (in this example) the spindle was actively cooled. The blue line shows the measurement results, while the red line is a fitted line assuming the exponential model

$$T(t) = T_\infty + a \cdot e^{-t/\tau}.$$

As a rule, the temperature is said to be stabilized after a period of 5τ, so in the example depicted in Figure 4 after a warming period of 34 hours.

3.6 Implementation and verification of the correction

To correct the geometric errors the machine tool controller must be equipped with correction software. Optimally this software allows a fully parametric correction according to ISO 230-1. This means, the component, location and orientation errors for the individual axes are processed by the machine tool controller according to the corresponding error model in order to calculate the correction for each point in the working volume and in dependence of the active tool length. However, some machine tool controller require that the correction data is given as a list of error vectors for discrete grid points in the working volume, calculated either by the measurement software or by additional software tools. In this case, the number of points per axis should not be smaller than for the measurement of the errors. Otherwise interpolation errors can occur. For the best results, the machine tool controller should be able to process also the rotational errors, in order to adjust the correction value to the actual tool offset. This means, for each point in the working volume a spatial error vector as well as three rotational errors must be given. If only the spatial error is processed by the controller, the correction table is only valid for a certain tool length. If the tool is changed, another correction table must be calculated.

After the correction table is implemented in the machine tool controller, a verification of the geometric error has to be performed. One way to do this is by measuring the residual errors, i.e. the geometric errors which remain after the correction. To this aim, the same measurement procedure as described above is repeated for the corrected machine tool. Note that in the case that the rotational errors are not processed by the machine tool controller, different correction tables for different reflector offsets have to be use. The so measured residual errors can then be used (among other influences) for task specific uncertainty calculation, say by a Monte-Carlo simulation.

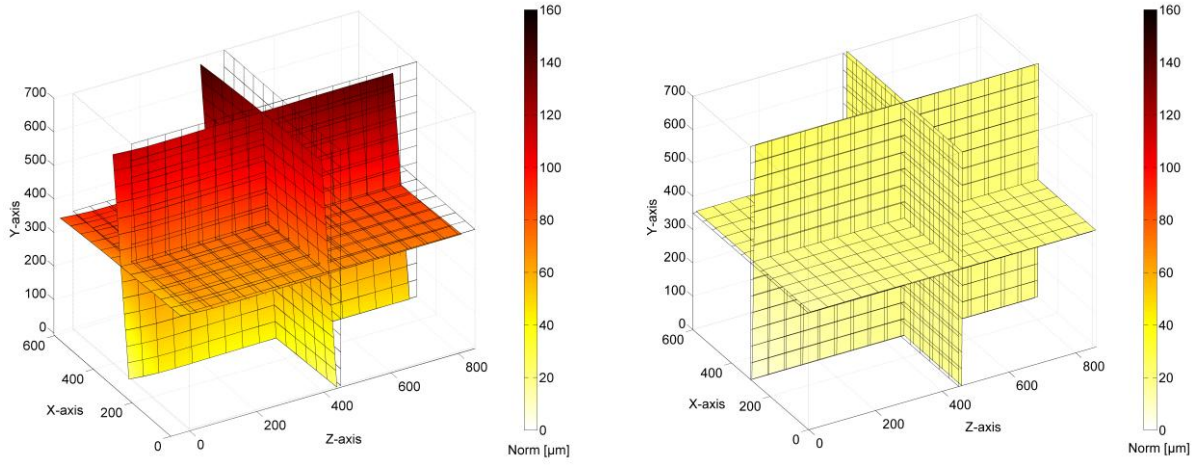

Figure 5: Geometric errors without and with geometric error correction (measured at 20 °C)

The improvement of the accuracy is illustrated in Figure 5. On the left are the colour-coded absolute values of the geometric errors for the uncorrected machine tool. The direction of the error is indicated by the deformation of the planes. On the right the same is depicted for the corrected machine tool. In this example the maximum error vector was reduced by about 80%.

Quick procedures for testing the volumetric accuracy of a machine tool are described in the Standard ISO 230-6 [2]. These methods allow a decision, if the MT meets its specification, but cannot be used for a correction of the MT. Measurement can be performed also by using a laser interferometer. Another possibility is the usage of calibrated ball bars as described in Section 5. Such test are also useful for checking the long-term stability of the machine tool.

4 Mapping of geometric machine tool errors by using the Hole Bar (LNE)

4.1 Description

Most of the existing material standards are developed for CMM calibration, except the ball plates, 1D-ball arrays, and Telescopic Magnetic Ball Bars. Hence, the touch probe clamped in the spindle axis of the machine tool (MT) represents the main limitation to use most of them. Moreover, the harsh environment (oil, chips, collisions, temperature drift, etc.) also reduces their integration in MTs. Some aforementioned material standards require too many positioning configurations to identify the 21 geometric errors of 3 linear axes structural loop. Thus, any automation of the calibration process becomes very complex since it requires several adjustments, and usually the calibration is handled manually. In addition, steel and ceramic material is commonly selected for these standards. Because these materials are sensitive to the variation of the surrounding temperature, they are non-adapted for interim MT checking or calibration during the production process in the manufacturing shop floor. In this section, a newly designed Hole Bar and its use is presented. Thanks to its new geometric pattern, it allows to identify 1 linear positioning error and 2 straightnesses of any linear mechanical guiding system of the MT just by 1 measurement of the Hole Bar. This identification of 3 parameters for one orientation of the Hole Bar leads to minimized MT's downtime. Furthermore, the combination of measurements performed on two parallel positions of the Hole Bar increases the number of identified geometric errors to 5 (1 linear positioning error, 2 straightnesses and 2 angular errors for each axis).
The material of the Hole Bar has to combine a small coefficient of thermal expansion (CTE), a high toughness and small brittleness in order that it can be used harsh environmental conditions as they occur on shop floors. Thus, Invar was chosen as the best candidate material.

The Hole Bar itself was calibrated on a traceable CMM at LNE. Therefore, the calibration of a MT using the Hole bar links its metrology traceability to the international traceability chain as illustrated in Figure 6.

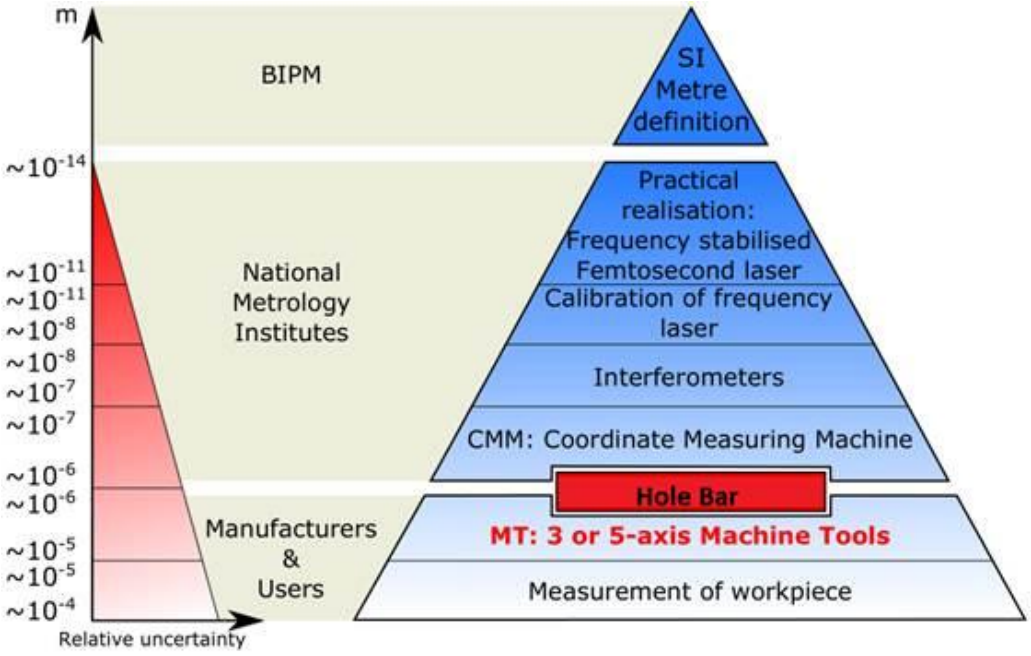

Figure 6: Integration of Hole-Bar in traceability chain to the SI metre definition

4.2 Concept of Hole Bar

The new design of the Hole Bar consists in a repetition of a 3D-pattern in one direction. Each pattern contains 7 features: 4 flat surfaces (vertical planes) and 3 cylinders (one vertical inner cylinder and two horizontal outer cylinders). The patterns repeated along the direction Δ as illustrated in Figure 7, where $1 \leq i \leq N$ and $1 \leq j \leq N - 1$. Once measurements on each pattern are carried out, the processing of the measured data allows extracting one point corresponding to the intersection of the 7 features mentioned previously. The expected measurements and the post-processing of the measured data can be completed with respect to the following steps:

- At least 8 points should be measured on each hole HOL_i with a touch probe, as shown in Figure 7 b. A nominal cylinder is associated to the 8 measured points by applying the least squares criteria. Thereafter, the intrinsic characteristics of each associated feature establishing the common datum shall be considered to determine the $AXIS_i$ as shown in Figure 7 b;
- At least 4 points should be measured on each flat surfaces PL with a touch probe, as shown in Figure 7 c. The post-processing of the measured dataset with the least squares plane association allows to define the associated integral feature (nominal plane PL_{Lj} or PL_{Rj});
- For each horizontal outer cylinder CYL_j, 12 points shall be probed as shown in Figure 7 d. The analysis of the measured data using the least squares method allows to determine $AXIS_j$;
- The points PL_j and PR_j are obtained mathematically and correspond to the intersection of $AXIS_j$ with both planes PL_{Lj} and PL_{Rj} as illustrated in Figure 7 e. The horizontal least squares plane PL_i is associated to the 4 points P_{Lj-1}, P_{Rj-1}, P_{Lj} and P_{Rj}. The last step consists in the identification of the point of interest O_i that corresponds to the intersection of $AXIS_i$ and PL_i;

For the manufactured Hole Bar with N = 12, this leads to (at least) 316 measuring points for one position of the Hole Bar.

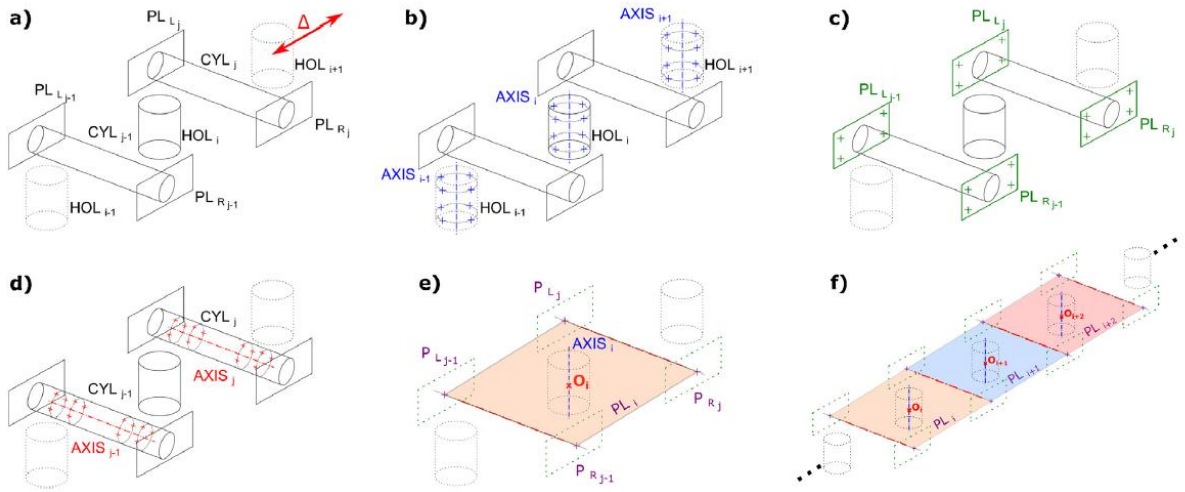

Figure 7: Principle of Hole Bar: patterns, probed points, and points of interest.

The 3D CAD model is depicted in Figure 8. This model is composed of 12 holes, thus it is possible to extract 12 points of interest O_i. The setting up of the MFB is ensured by using isostatic work holder built from modular equipment system.

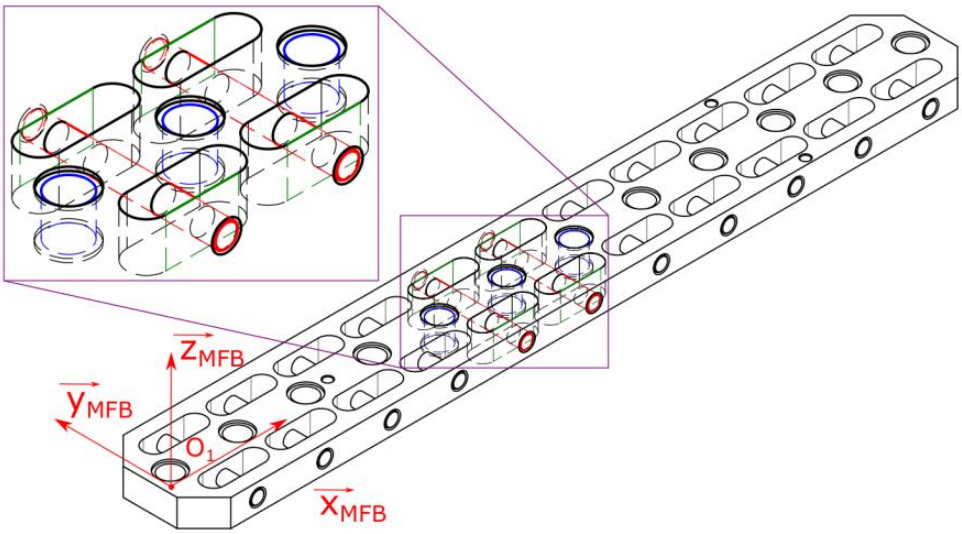

Figure 8: 3D CAD model of the Hole Bar

4.2.1 Handling

Note:

1. Use of gloves is strongly suggested for any handling of the Hole Bar to avoid any damage of the functional surfaces.
2. No gloves are required for the assembly of the other parts: plate and modular inspection equipment system.

- The fixture system can be performed in a short time with simply modular inspection equipment system.
- Common tools are required for the assembly such as:
  1. Hex keys for modular equipment
  2. Torque wrench to tighten up the Hole Bar on the work holder through four nuts.

All tools necessary for the assembly are provided in the transport case.

The mass of the material-standard and the different other elements are listed in the following table:

Parts	***Mass [kg]***
Plate	~ 10.5
Hole Bar	~ 5
Modular inspection equipment system	~ 2
Total (Hole Bar + Work Holder)	~ 18

Table 1: Mass of the material-standard and the different other elements

Some dashes of grease can be visible in some zones of the Hole Bar. For this reason, the Hole Bar should be cleaned with a solvent before any use. However, the Hole Bar can be immersed long time in a solvent to avoid any damaging of the glue used to fix the rods in the Hole Bar.

4.2.2 Assembly

The goal of this system is to maintain the orientation of the Hole Bar fix during the measurement and to provide an isostatic setting up of it. The system allows mounting the Hole Bar along each of the three axis. The realization of this assembly as illustrated in Figure 9 is essential. In particular, it allows calibrating the hole in a similar condition as it is used on machine tools. Furthermore, two black

handles are provided in the same transport case. The use of these handles is helpful for handling the whole system including the holder system together with the Hole Bar.

During the tightening, it is necessary to insure that a contact is well established between the washer, the sphere and the mounting flange. Normally, the washer does not move after tightening. The tightening torque applied on the four nuts must absolutely be equal to 1.5 Nm. In addition, the nuts should be embedded gradually.

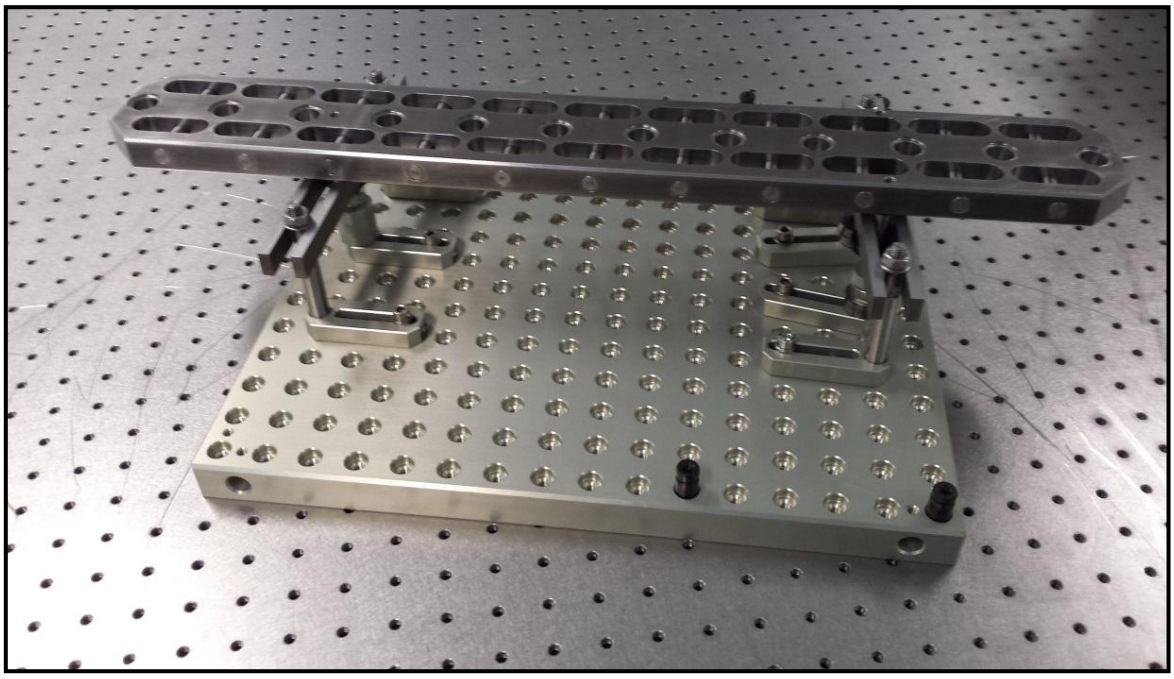

Figure 9: Work Holder and Hole Bar - horizontal setup

4.3 Machine tool checking

At the beginning, the Hole Bar should be aligned along the selected axis. The alignment of the Hole Bar along the selected machine tools axis should be precise to less than 0.1 mm (Figure 10). The alignment can be easily checked by measuring one point in one side and a second point in the opposite side. This operation should be done along the two orthogonal directions to the selected machine tools axis. For example, if the selected axis is the X-axis, then the verification of the alignment should be done along the Y and Z axes.

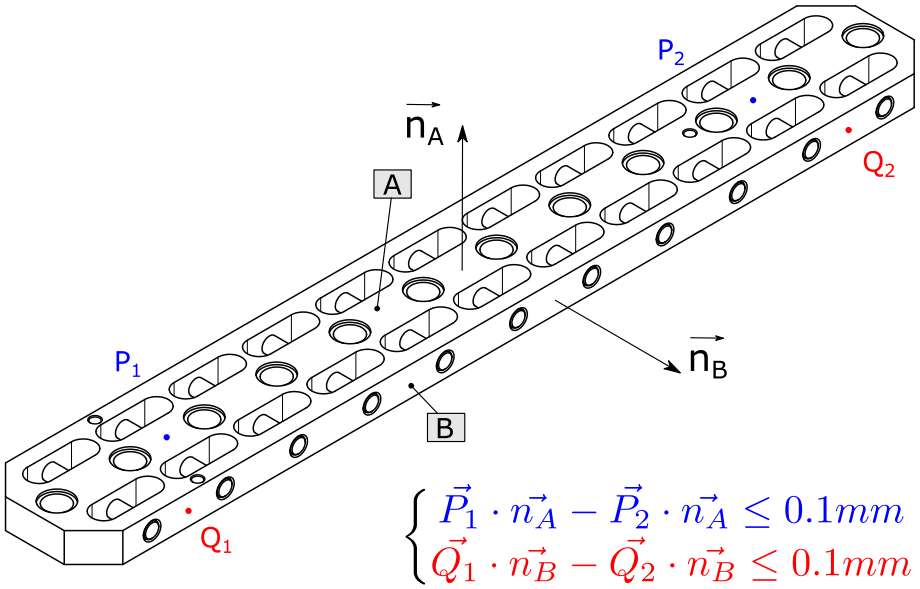

Figure 10: Alignment of the Hole Bar along the selected axis

4.3.1 Building of the local frame

A local frame is built by probing the three planes A1, B, C (with a minimum of 3 points for each plane). Let $\vec{n}_{A1}$, $\vec{n}_B$, $\vec{n}_C$ are the outer-pointing normal vectors of the plane A1, B, and C, respectively. The intersection of the 3 planes is the point J. From J one can define the origin O of the local frame and the axes as depicted below:

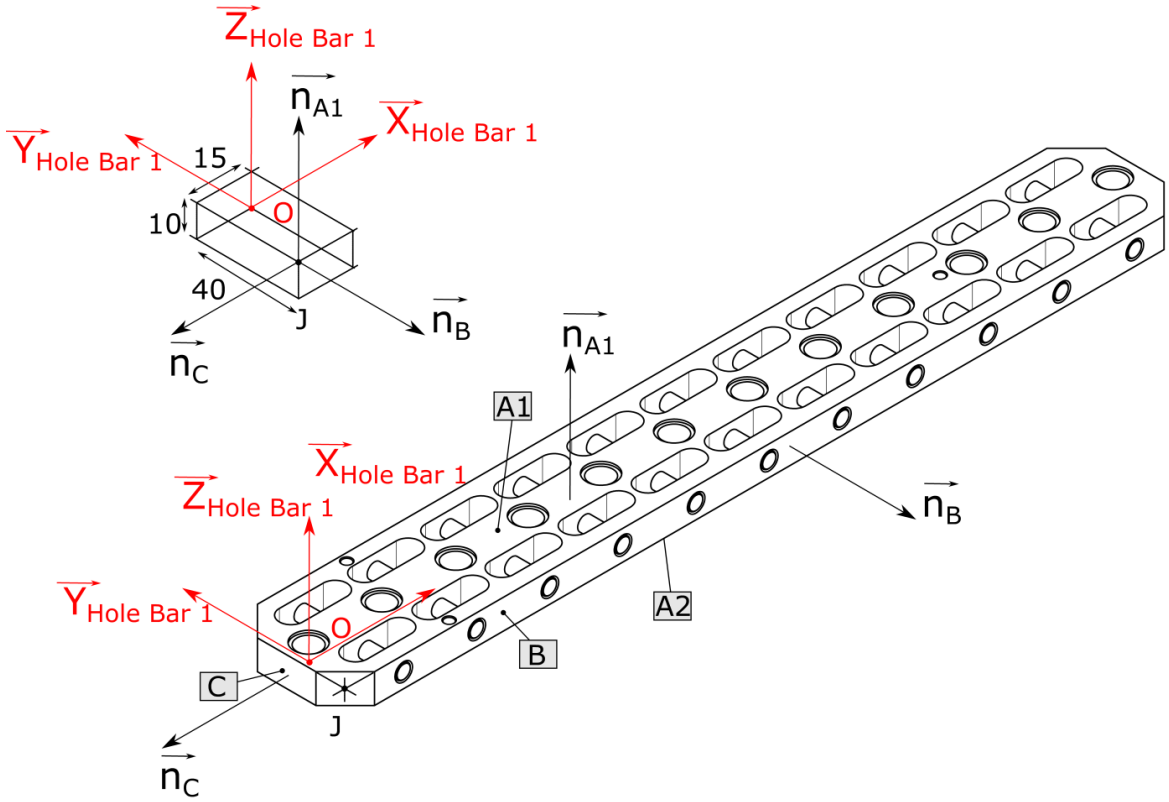

Figure 11: Building of local frame of the Hole Bar

The origin O corresponds to the intersection of the median planes of the Hole Bar and the axis of the first nominal hole, as in Figure 11.

4.3.2 Required position for geometric errors identification:

The next figures (Figure 12, Figure 13, and Figure 14) depict the different positions which are required to perform the identification of geometric errors of linear axes. This summary does not include diagonal measurements. The identification of angular motion errors can be carried out by differential measurement of straightness errors or linear positioning errors. This technique is depicted in ISO230-1 and represented by a substractor symbol.

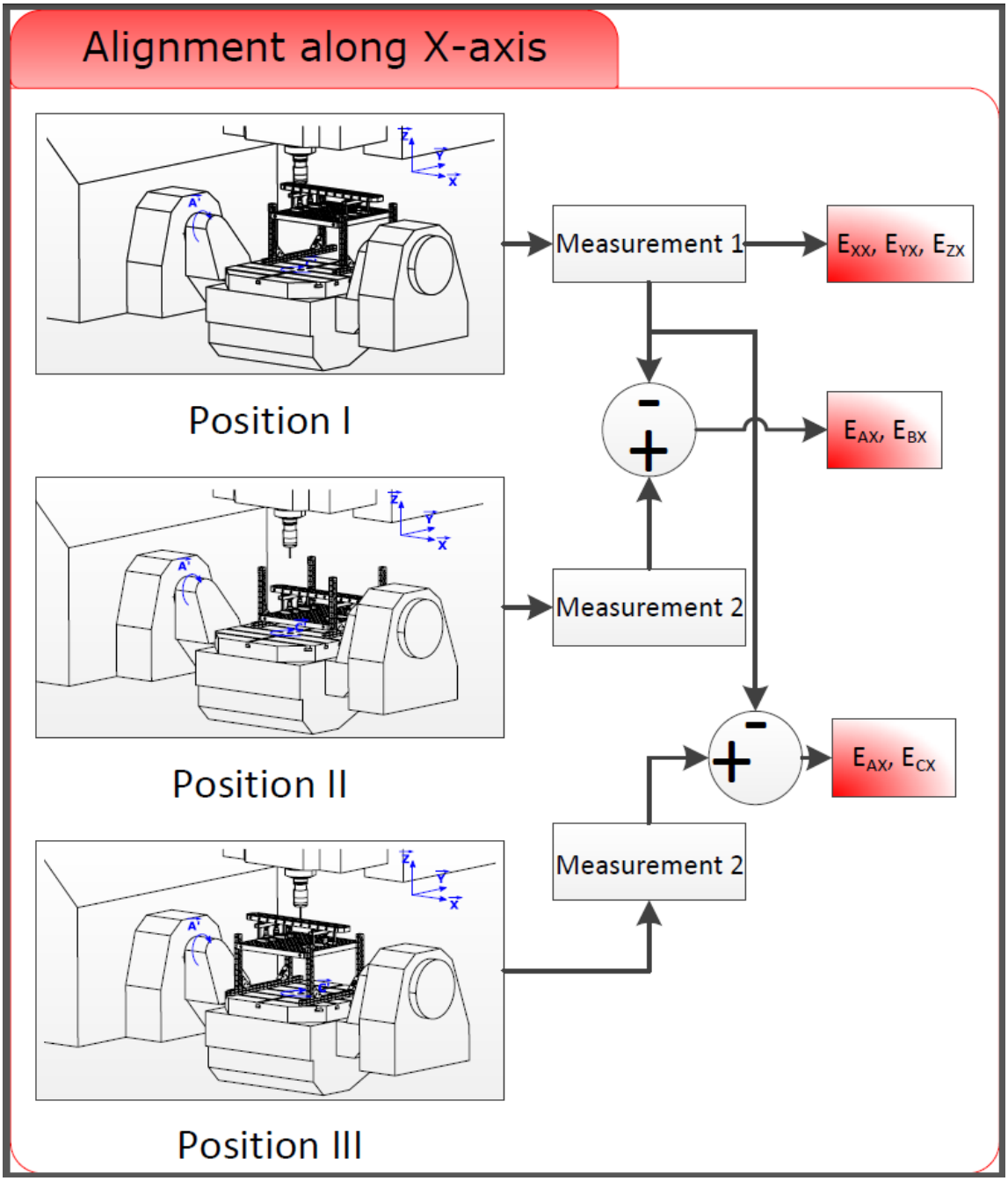

Figure 12: Required positions of Hole-bar to identify geometric errors of X-axis

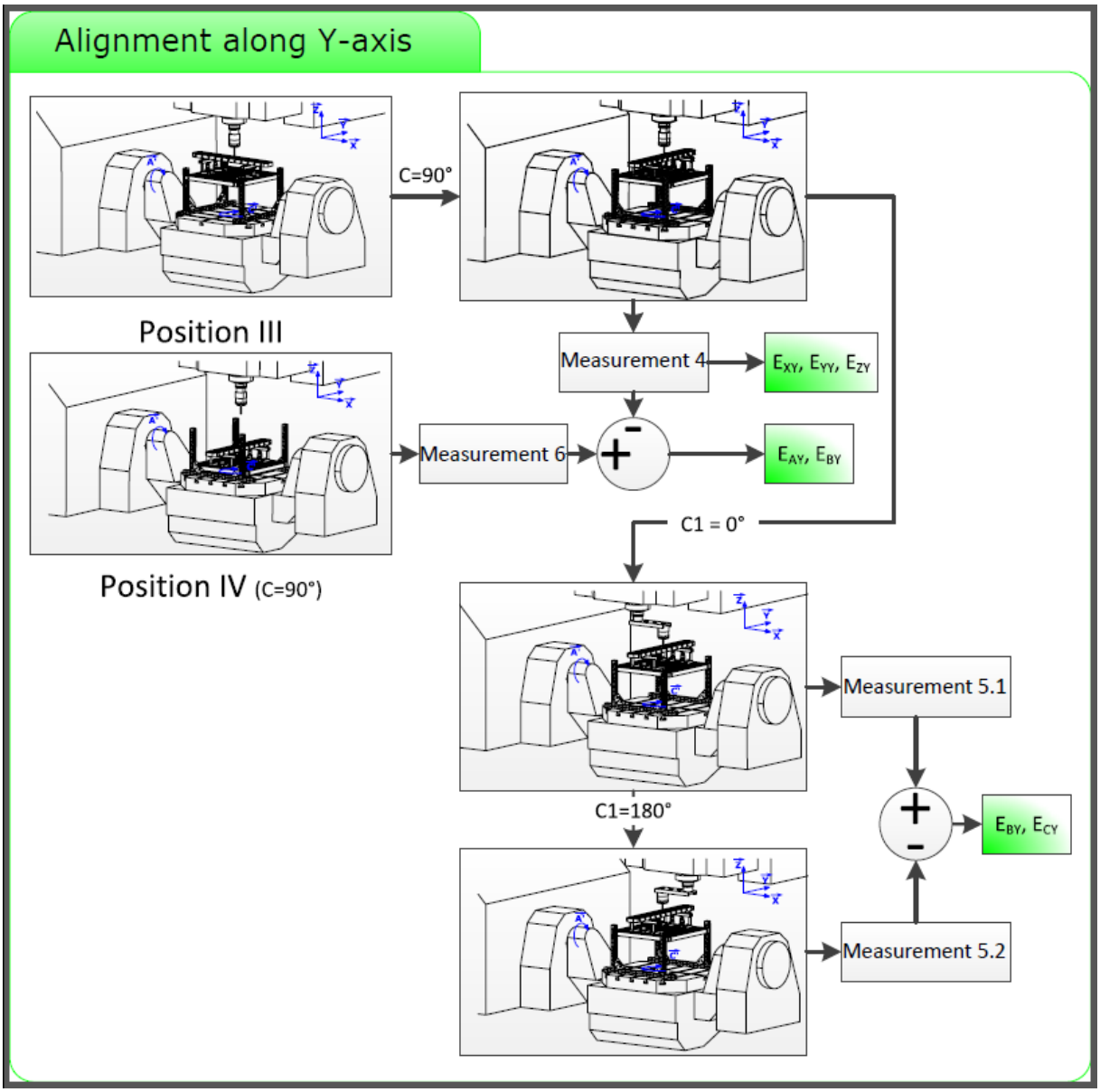

Figure 13: Required positions of Hole-bar to identify geometric errors of Y-axis

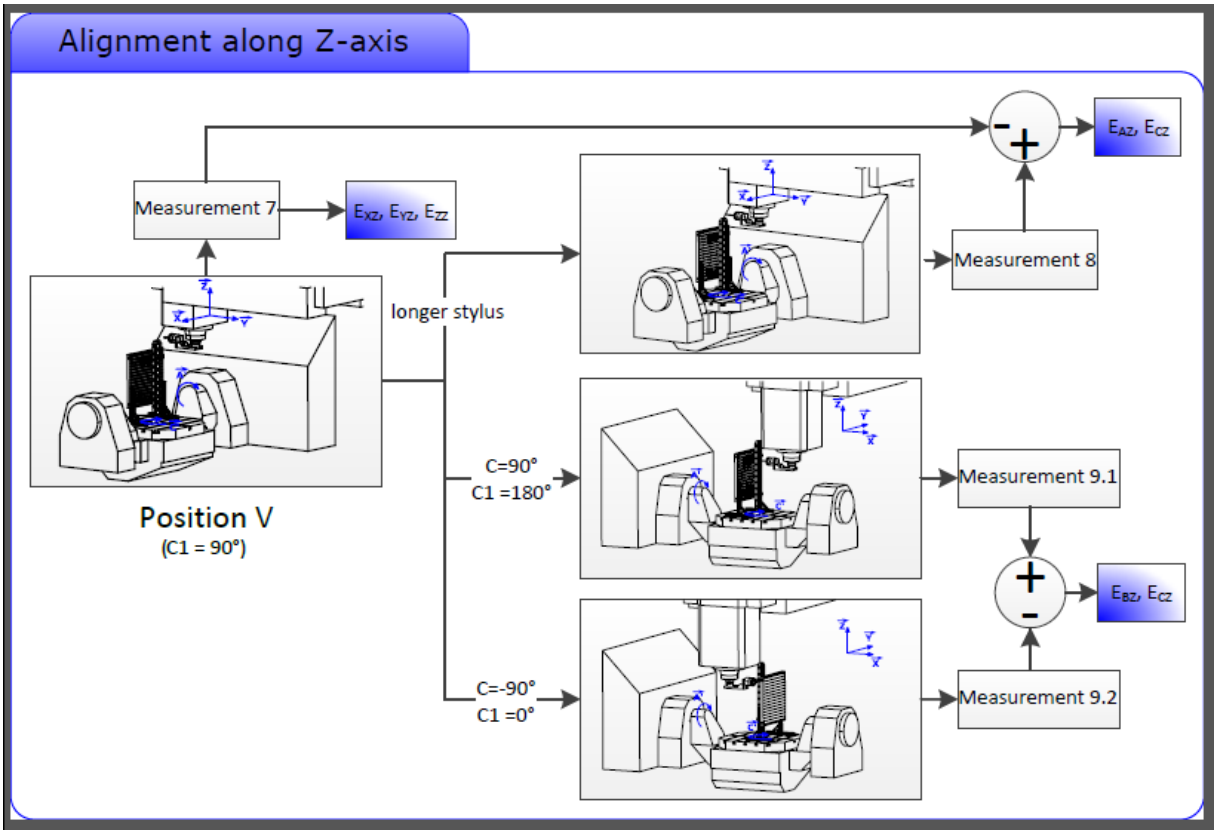

Figure 14: Required positions of Hole-bar to identify geometric errors of Z-axis

4.3.3 Measurement process

The following pictures show all the different setting-ups of the 3D-Hole bar, which are necessary for the identification of the 21 geometric errors of the 3 linear axes for a structural loop, including diagonal measurements. In each position, 316 points on the hole bar have to be measured. A Matlab software has been developed to generate the NC code for the measurement. This code can be executed in the machine tool to measure the 316 points and record them directly by a developed Matlab interface.

The identification of the geometric errors can normally be evaluated in 1 day, including adjustments, measurements, acquisitions and data exploitation. The pictures show the use of the 3D-Hole bar on a Mikron UCP710 5-axis machine tool.

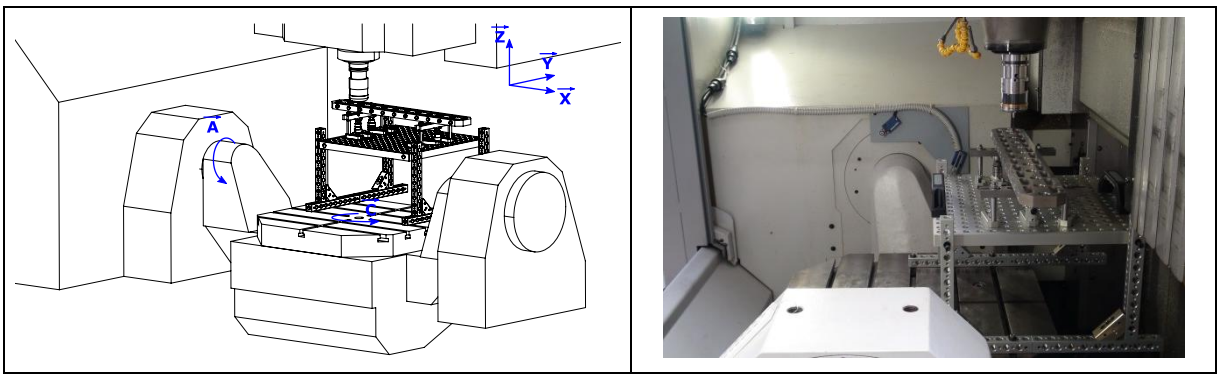

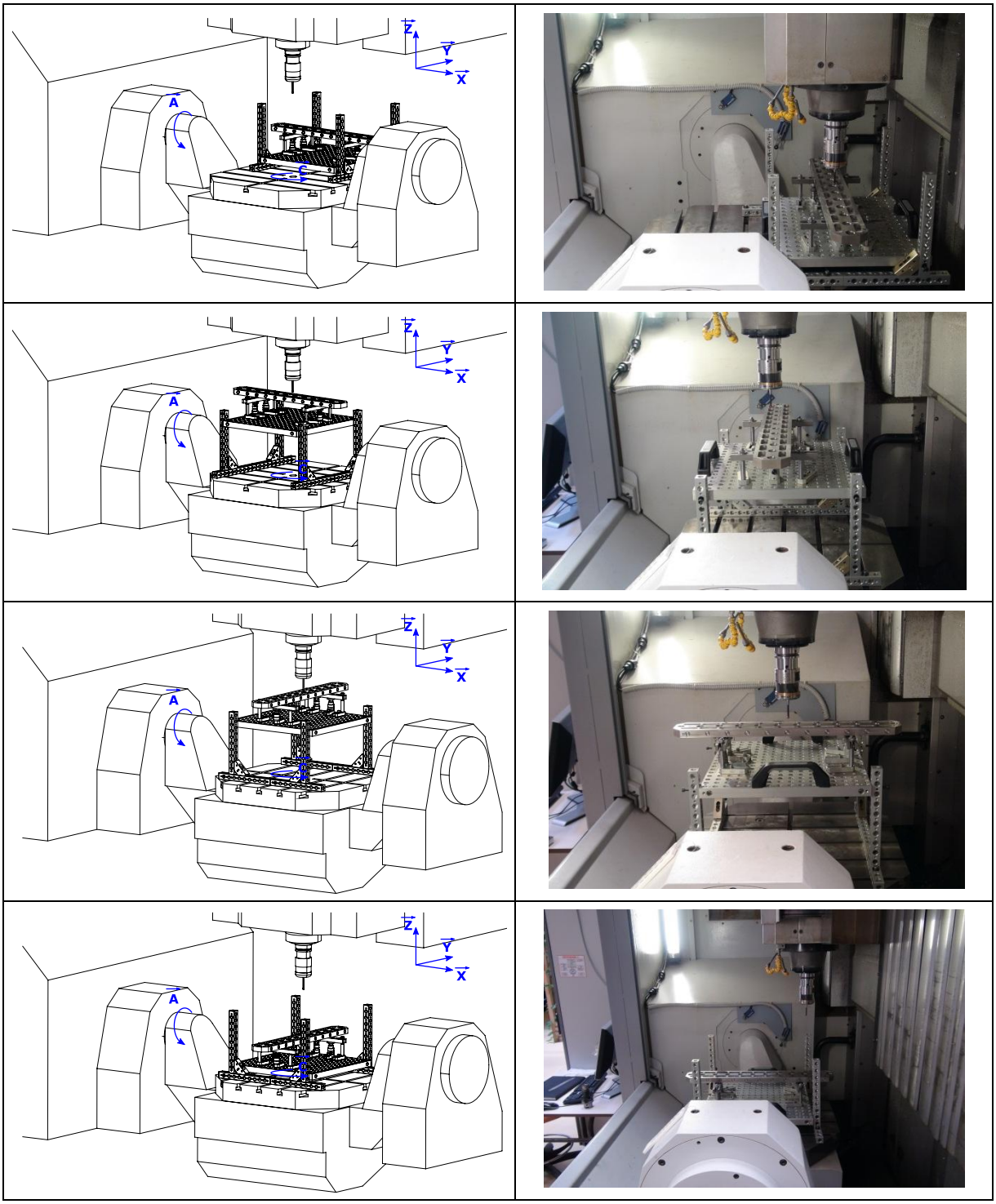
Z
Y
X
A
C

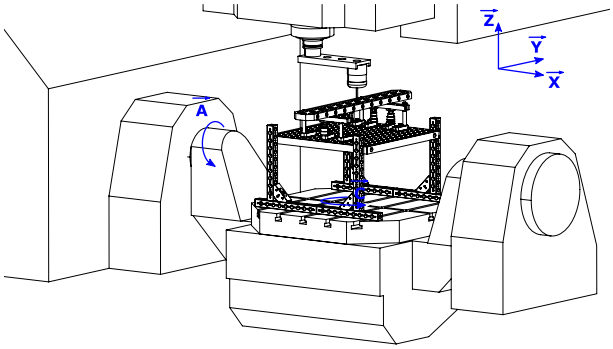 Z Y X A	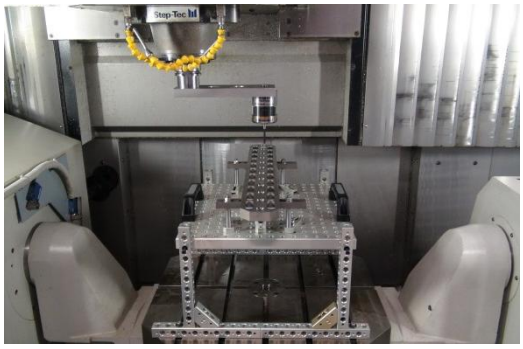
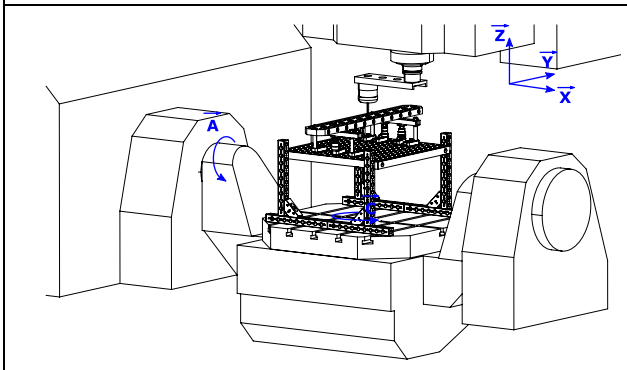 Z Y X A	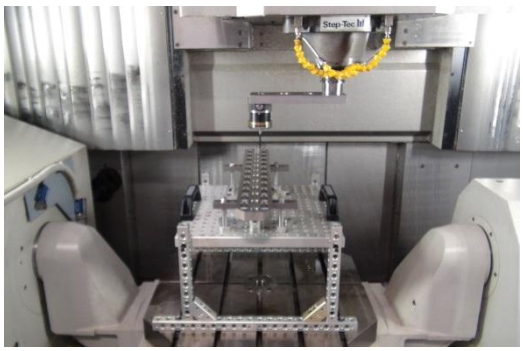
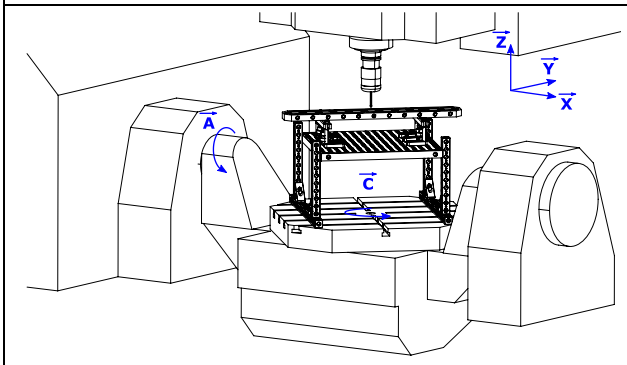 Z Y X A C	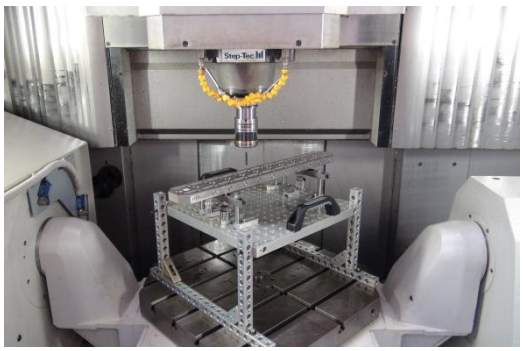
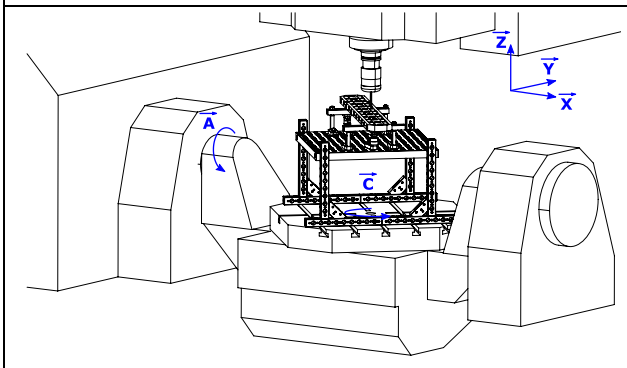 Z Y X A C	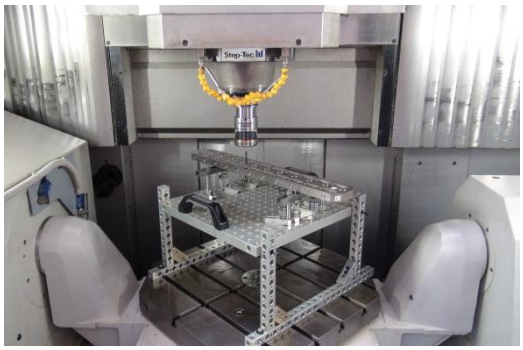

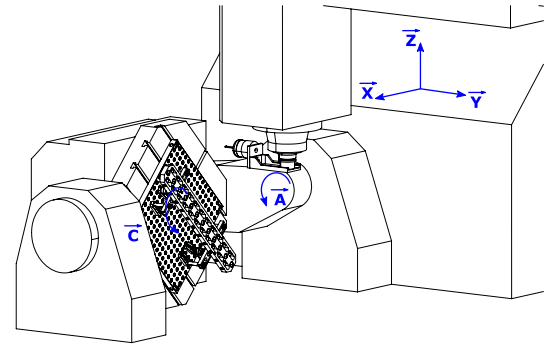 Z X Y A C	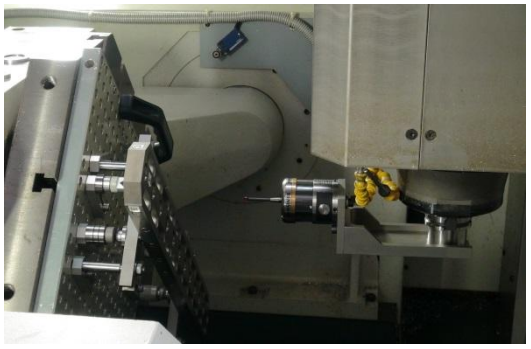
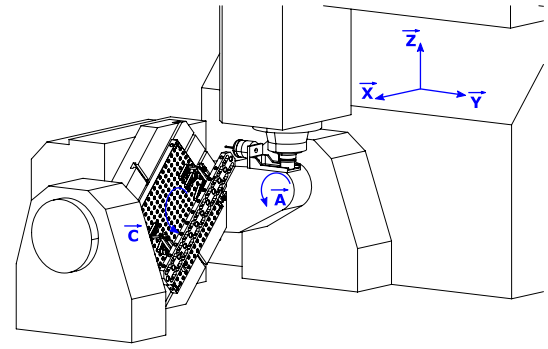 Z X Y A C	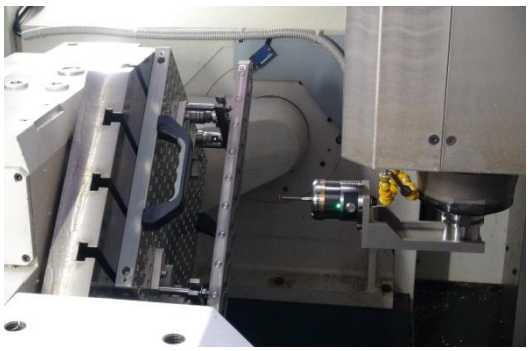
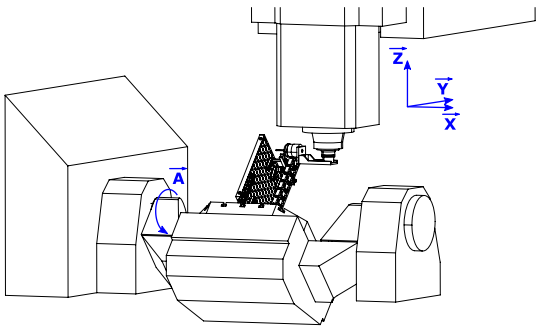 Z Y X A	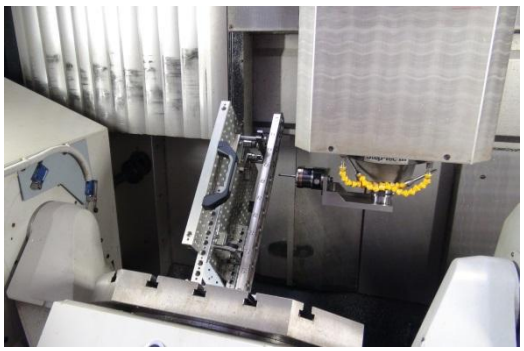
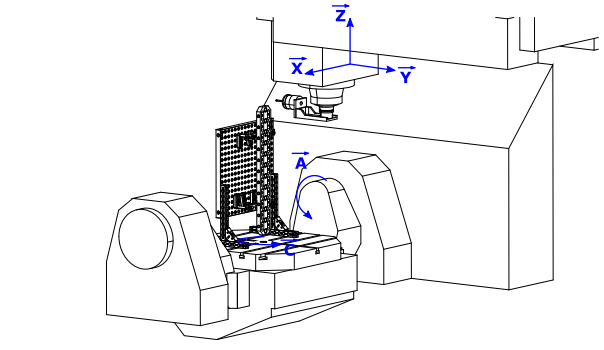 Z X Y A C	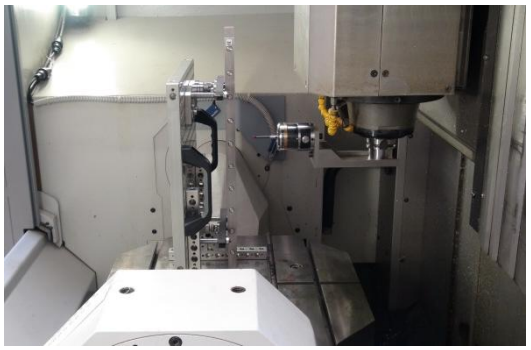

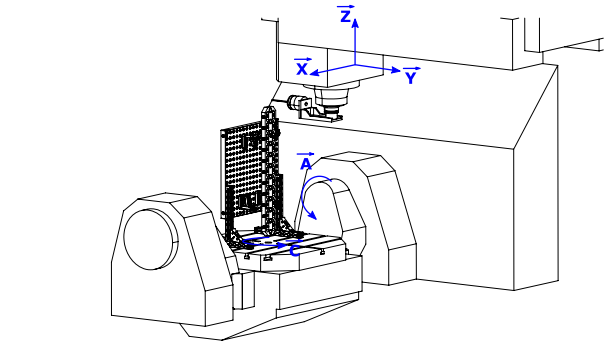	
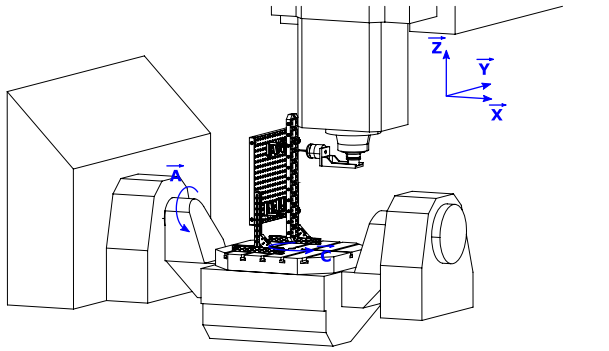	
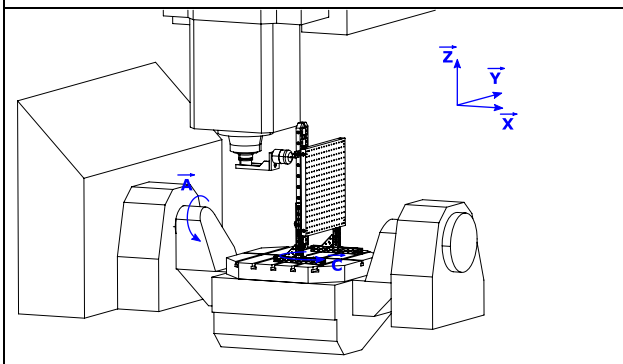	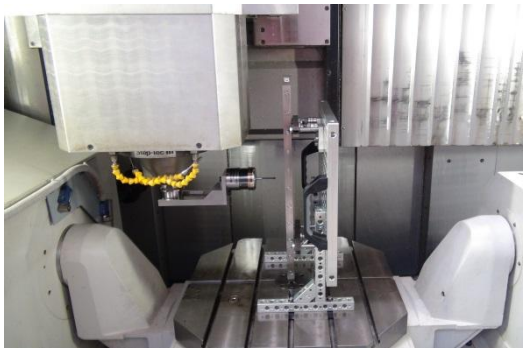

Table 1: Different positions of the 3D-Hole bar on the Mikron UCP710 machine tool

This entire procedure is carefully detailed in the developed Matlab program (i.e. there are questions, description of the instructions, and some request user input in the command windows of the software). The 3D deviations between the measured points of interest O_i of the Hole Bar using the machine tool and the calibration results of the calibration of the Hole Bar on an accurate and traceable CMM can be calculated. The 3D deviations correspond to the position components of the volumetric error. Thus, the position components enable to assess measurement performance of machine tools.

An end user interface developed on ControlDesk software (Figure 15) for performing the measurements on machine tools is available.

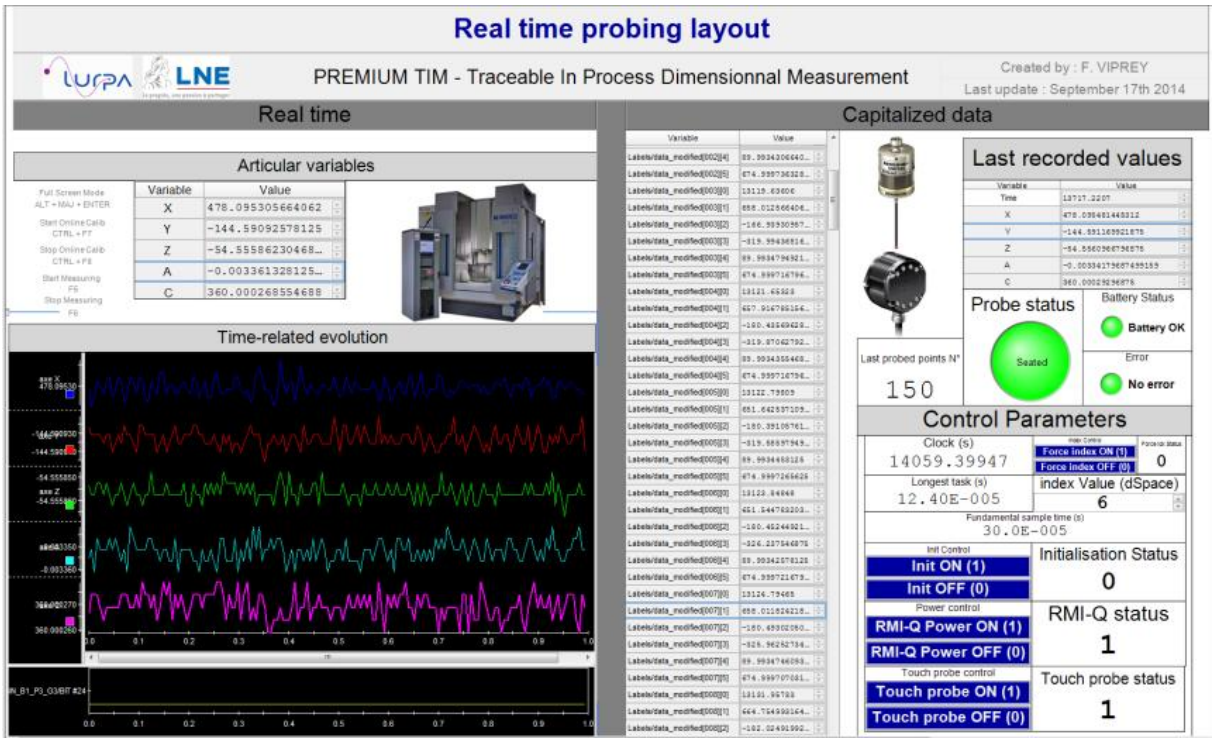

Figure 15: End user interface to perform 5-axis on-line measurement in real time

4.3.4 Measurement results

For the identification of the 21 geometric errors from the measured point coordinates, a Matlab algorithm is used. In Figure 16, Figure 17, and Figure 18 results obtained for measurement of the X-axis of a MT (Mikron UCP710) are presented. The identification of the straightnesses (Figure 17) is performed from the end-point reference straight line. The straight line connects the first and the last points of the measured straightness deviations.

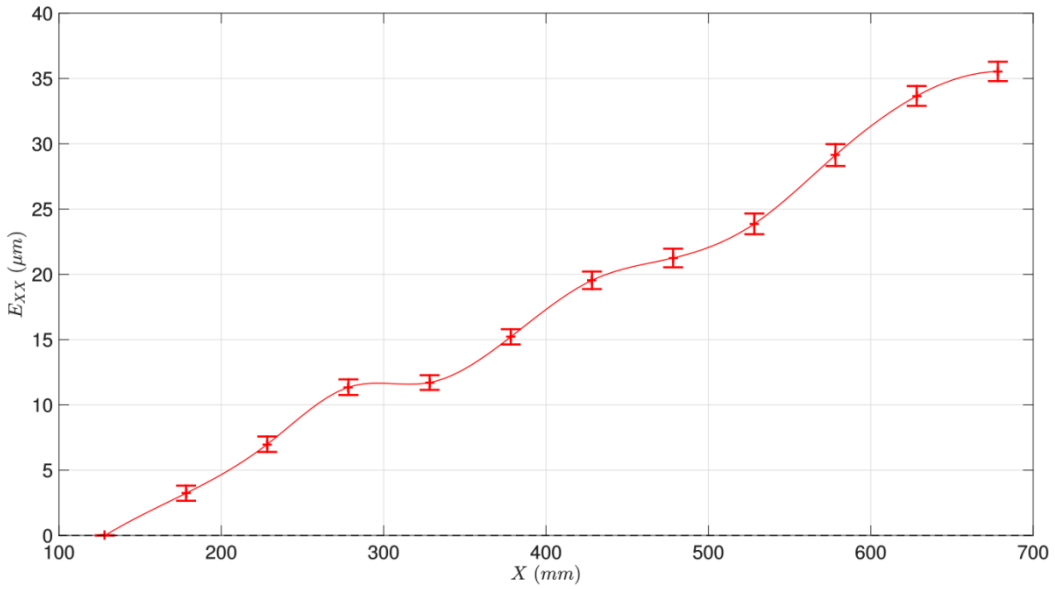

Figure 16: Linear positioning error of X-axis: E_{XX}.

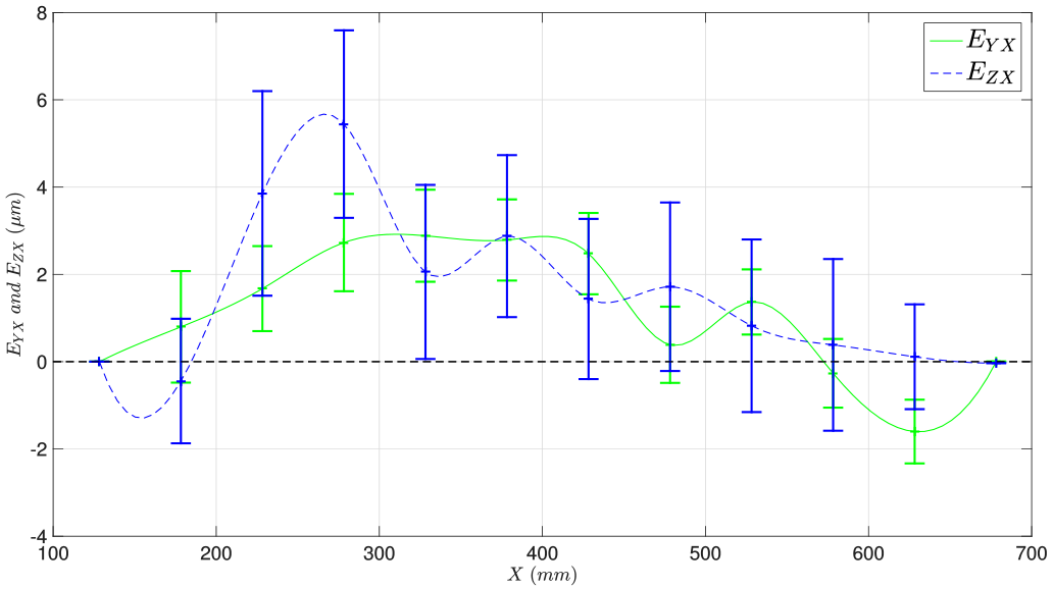

Figure 17: Horizontal and vertical straightness of X-axis: E_{YX} and E_{ZX}.

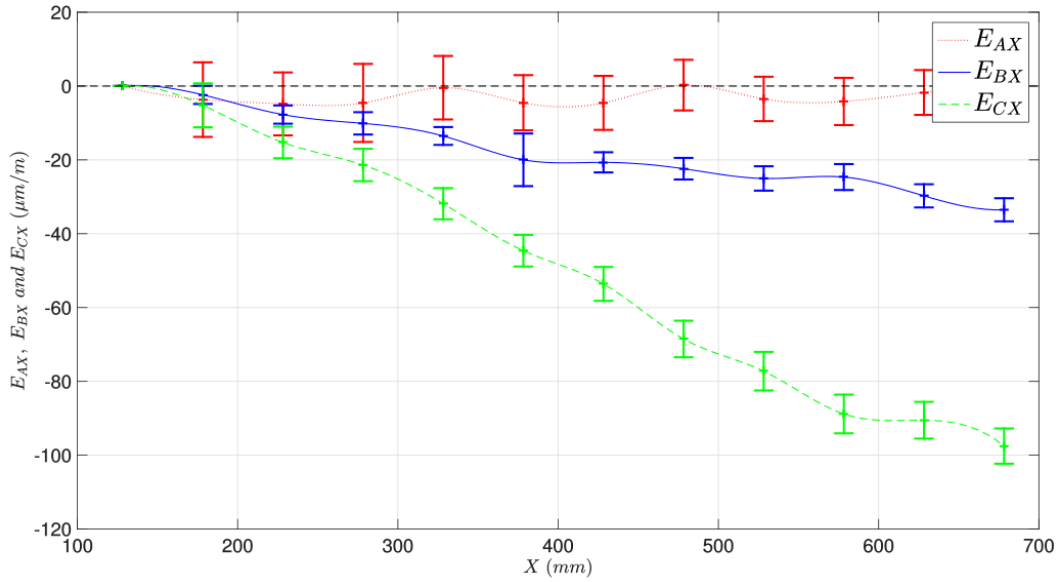

Figure 18: Roll, pitch and yaw of X-axis: E_{AX}, E_{BX} and E_{CX}.

4.3.5 Uncertainty

For the calculation of the uncertainties of the geometric errors, a Monte-Carlo simulation can be performed. The following uncertainty contributions are considered:

- measurement reproducibility including the resolution of the measuring device, the repeatability of touch probe, the random motion error of each MT-axis, vibration, thermal drift,
- position and orientation errors of the Hole-Bar in the MT-workspace,
- offset components errors of the touch probe,
- traceability chain of the Hole-Bar including the calibration process, the application of the reversal technique, the clamping system and CMM traceability,

In Figure 16, Figure 17, and Figure 18, the error bars represent the uncertainty the so derived uncertainty. Finally a C^2-spline interpolation of the measured geometric errors provides a potential accurate compensation models for E_{XX} , E_{YX} , E_{ZX} , E_{AX} , E_{BX} and E_{CX}.

4.4 Work holder for positioning of Hole Bar

4.4.1 Horizontal positioning of Hole Bar

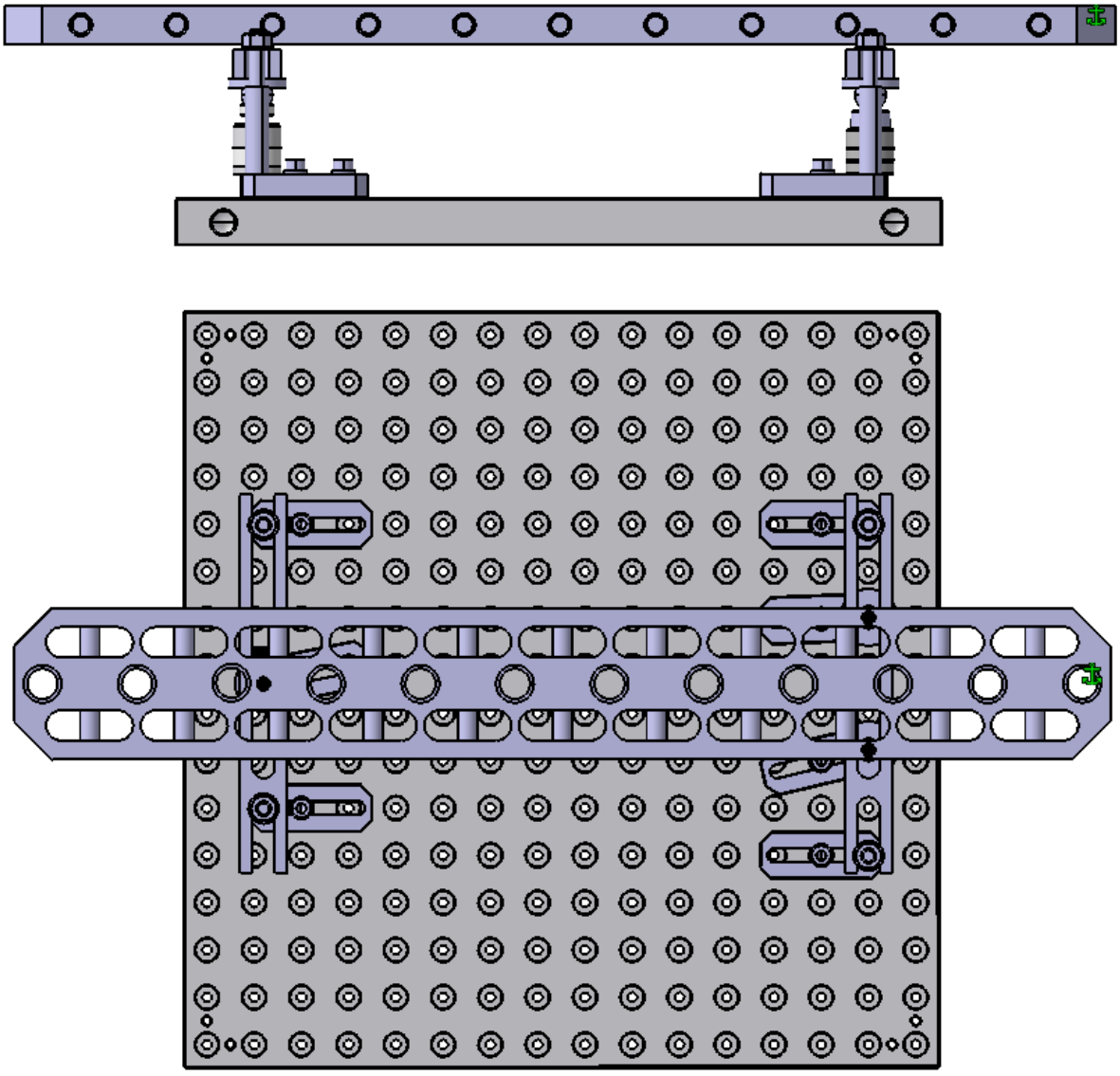

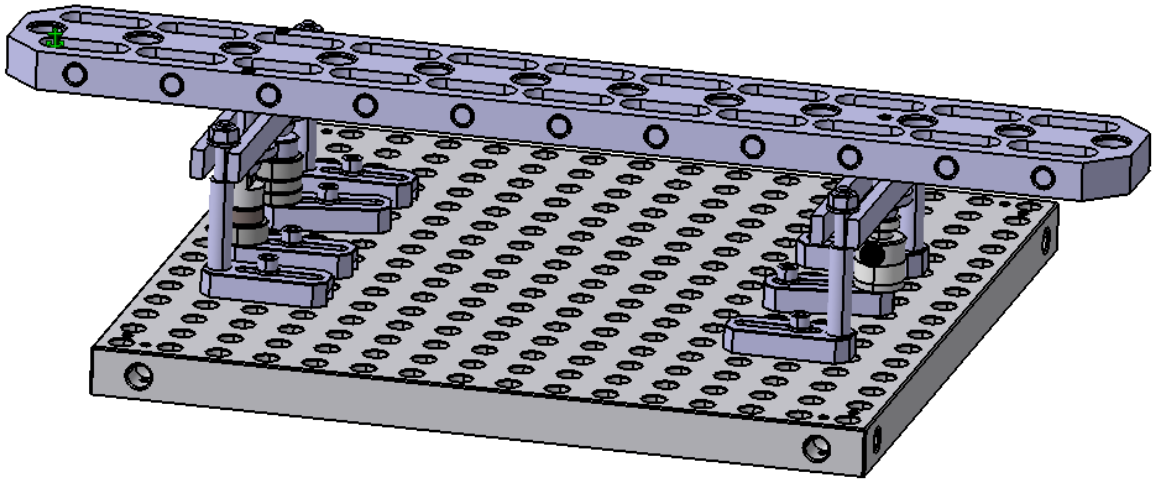

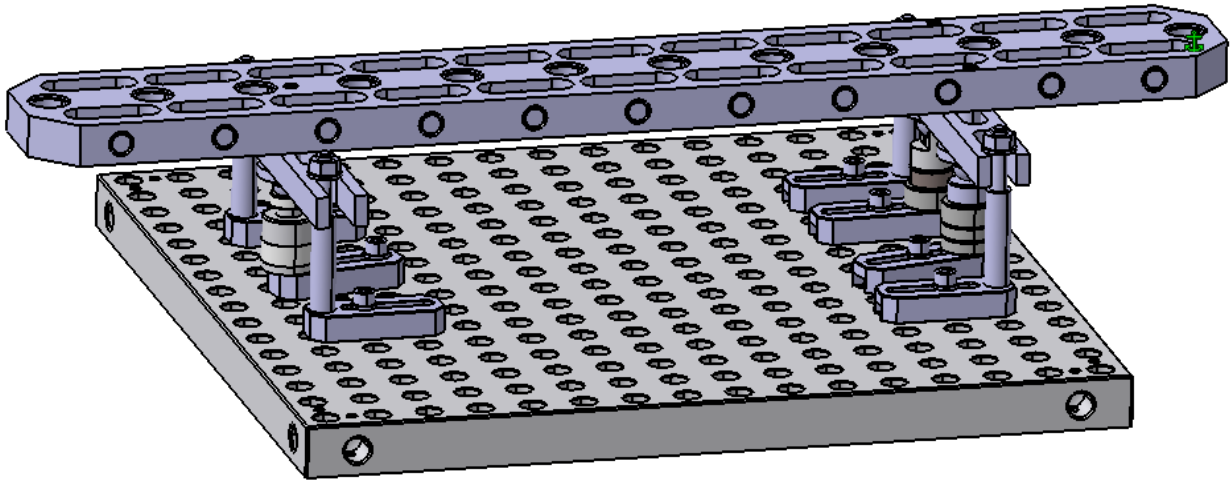

4.4.2 Vertical positioning of Hole Bar

N.B: It is the same work holder which is presented in Subsection 4.4.1, the frame features is equipped with two T-base.

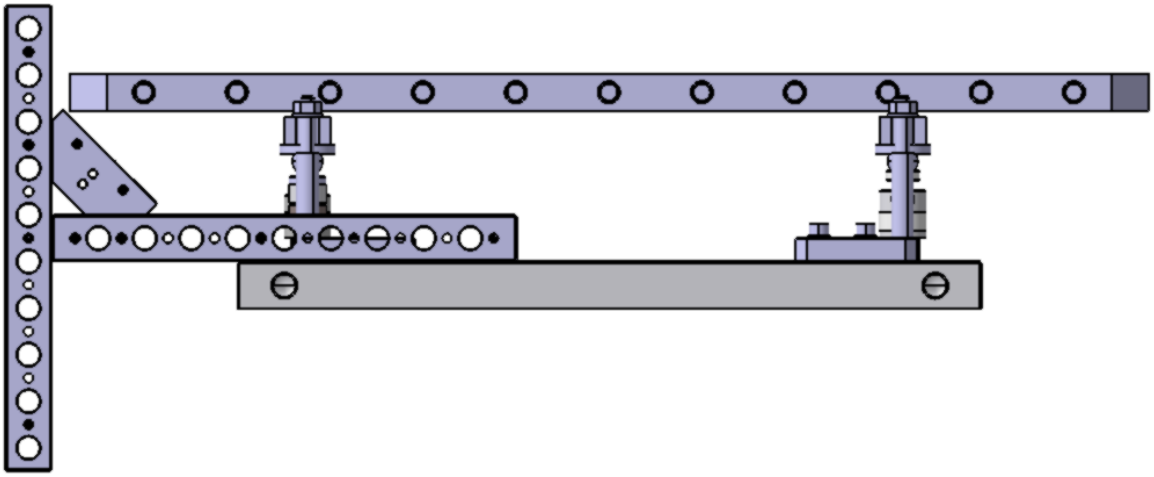

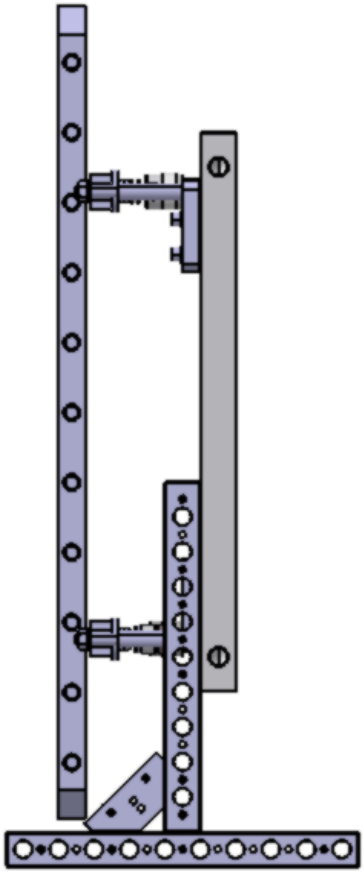

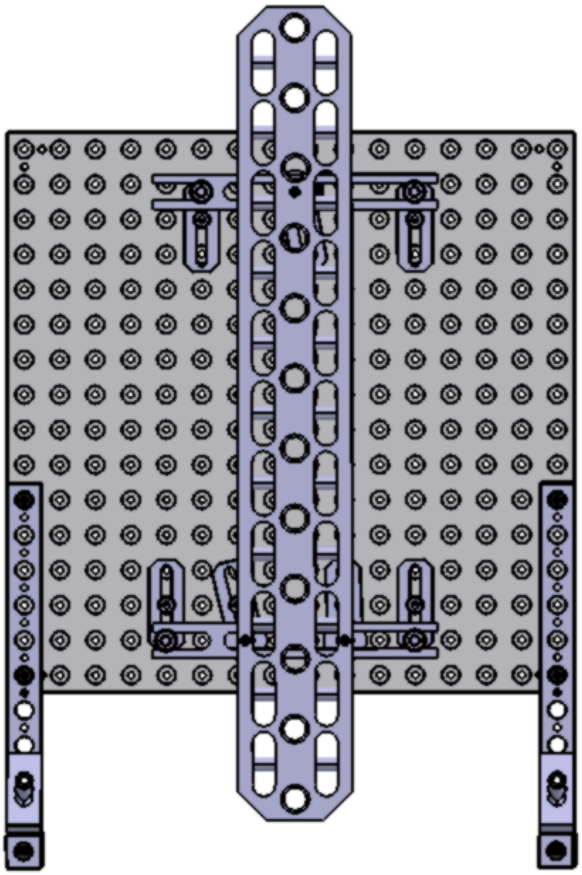

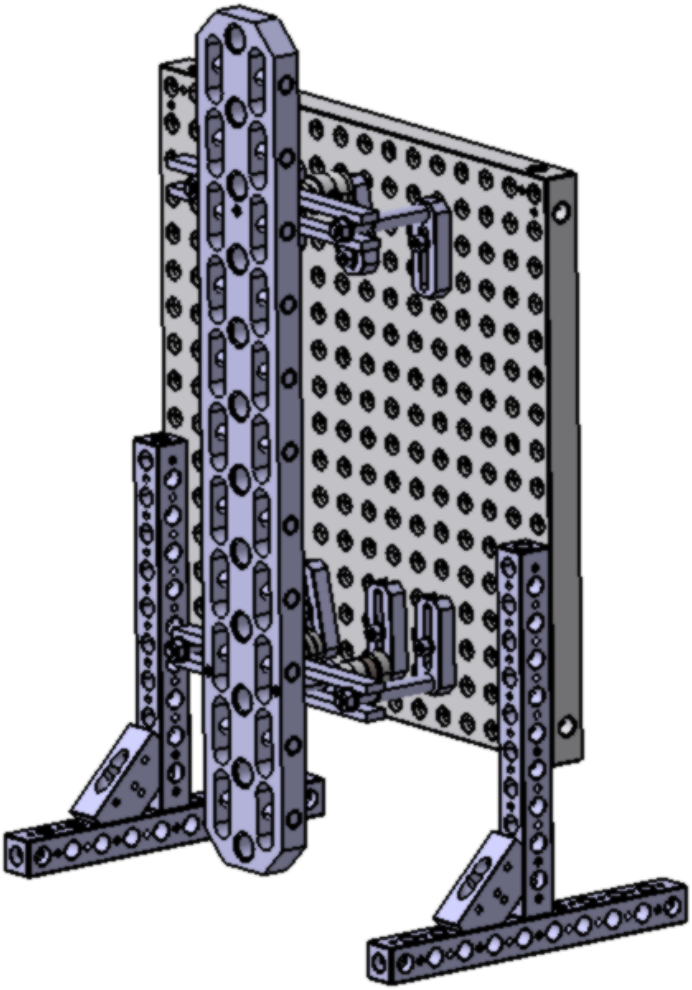

5 Checking the measurement performance by using ball bar standard (UM)

5.1 Introduction

This procedure describes steps for checking geometrical machine tool errors in three linear axes in order to verify the performance of 3D length measurements on the machine tool according to ISO 230-6 [2]. A 1D ball bar is used as the standard in this performance test. The standard is thermally invariant and therefore applicable in any shop floor environment. It is available in two lengths: 500 mm and 1000 mm with one extension, which can be combined with this two base standards to generate additional lengths of 1500 mm and 2000 mm. Calibrated ball standards consist of two ceramic spheres/balls, steel joints and a body made of composite material (Figure 19). Ceramic spheres with a diameter of 30 mm and roughness below 0.2 µm are used as probing elements.

Figure 19: Ball bar standard

The aim of the verification procedure is to evaluate performance of 3 and 5 axes milling machines. The verification is enabling the end users to determine whether the machine tool is appropriate for their specific requirements or not, whether the maximum measured length error is smaller than maximum permissible length error (MPE).

Prior to conducting performance test, the ball-standard must be mounted on the machine tool table by using the clamping elements and the tripod (Figure 20) in accordance with specifications provided by the manufacturer and ensuring suitable mounting stiffness and orientation. Moreover, appropriate environmental, electrical and vibration conditions must be provided during the entire process.

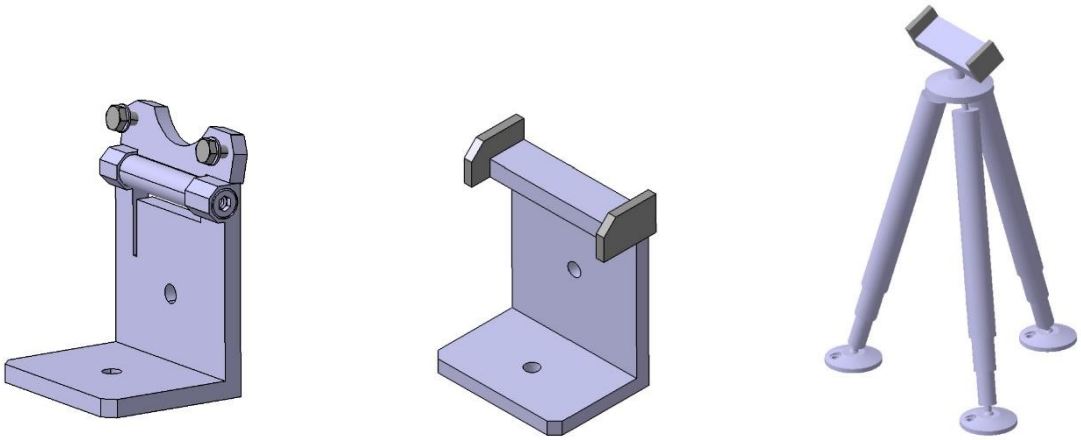

Figure 20: Clamping elements

5.2 Visual check and cleaning

The material standard is to be visually checked for any obvious defects (e.g. scratches), which could impede the test. Ceramic balls should be cleaned with alcohol, when necessary. The clamping elements and the machine table must be cleaned to ensure proper mounting of the ball standard to the machine table.

5.3 Temperature stabilisation

The standard shall be stabilized at the measurement place for 30 minutes in order to assure homogenious temperature through the whole standard (thermal compensator inside the standard shall have equal temperature as the body of the standard in order to assure proper thermal expansion compensation).

5.4 Temperature measurement

In order to evaluate the temperature influences, temperature sensors should be placed on the ball standard and into the machining space to record the temperature on the ball standard and the air temperature inside the machine.

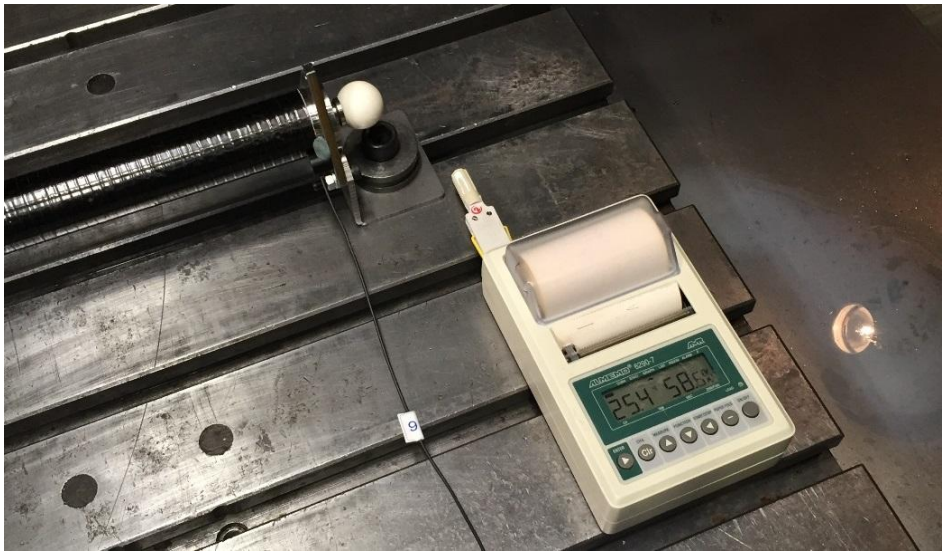

Figure 21: Temperature measurement

5.5 Touch probe

5.5.1 Milling centres without measuring system

In order to perform the verification test by using the ball bar standard, a machine tool shall be equipped with a 3D touch probe. The 3D touch probe is clamped into a tool holder and inserted into a milling spindle. Once clamped into the machine spindle, the 3D touch probe shall be set to zero.

Figure 22: Example of "simple" 3D touch probes

5.5.2 Milling centres with integrated measuring system

The touch probe is attached to the machine tool in the same way as in Section 5.5.1. Once clamped into the machine spindle, the 3D touch probe is calibrated with the calibration programme, integrated in the machine tool.

Figure 23: Example of an "active" 3D touch probe

5.6 Ball standard – combination

The ball standard is designed as a modular ball-bar artefact (2 standards + 1 extension) that can be combined in 4 different lengths:

- 500 mm standard (Module 1)
- 1000 mm standard (Module 2)
- 1500 mm (standard 500 mm + extension 1000 mm)
- 2000 mm (standard 1000 mm + extension 1000 mm)

The standard modules of the ball standard are fixed to the extension with the 3 screws.

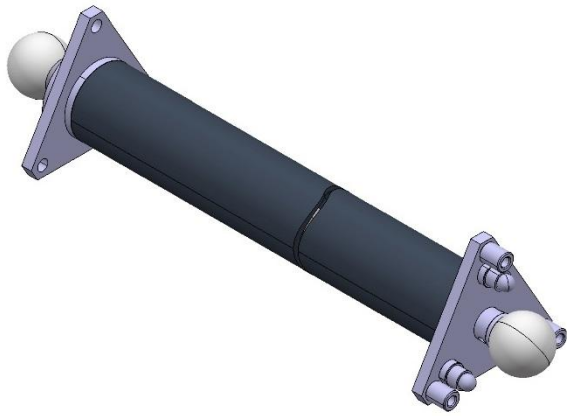

a) 500 mm standard (Module 1)

b) 1000 mm standard (Module 2)

c) 1500 mm standard (Modules 1+3)

d) 2000 mm standard (Modules 2+3)

Figure 24: Ball standard - combination

5.7 Testing procedure – 3 axes milling centre (fixed machine table)

5.7.1 Choosing the right standard

Table 2 is stating recommendations for using the standard according to the size of the working table on the milling centre.

Table size (X, Y, Z axis) in mm	Ball-standard length in mm
from 600 to 1000	500
from 1100 to 1500	1000
from 1600 to 2000	500 + extension 1000
from 2100 to 3000	1000 + extension 1000

Table 2: Recommendations for applying different ball bar lengths

5.7.2 Positioning the standard

Standard shall be mounted on the machine working table according to Figure 25, Figure 26 and Figure 27:

- For evaluating the “X” axis scale, the ball standard is set horizontally and placed parallel to the x axis. It is mounted by using special clamping elements shown in Figure 20.

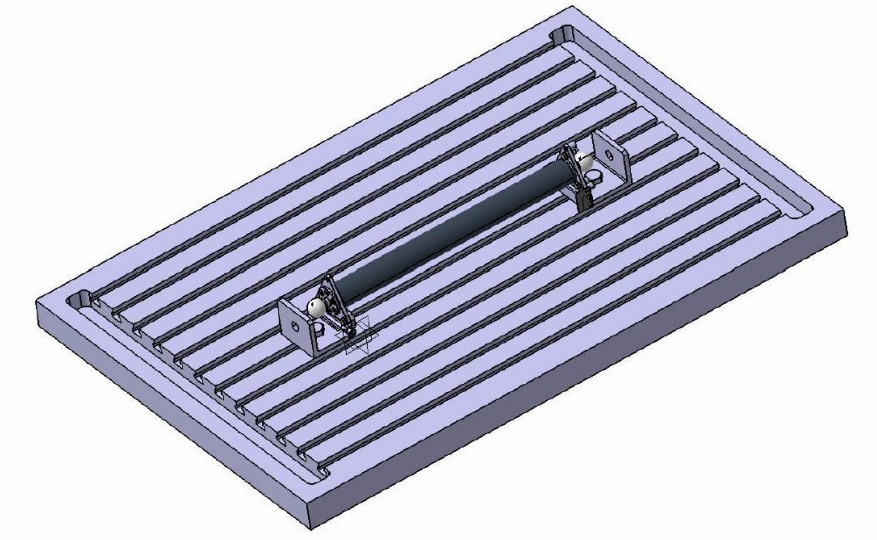

Figure 25: Position of the ball bar in X-Axis

- For evaluating the “Y” axis scale, the procedure is the same as for the “X” axis, but the ball bar is rotated by 90 degrees.

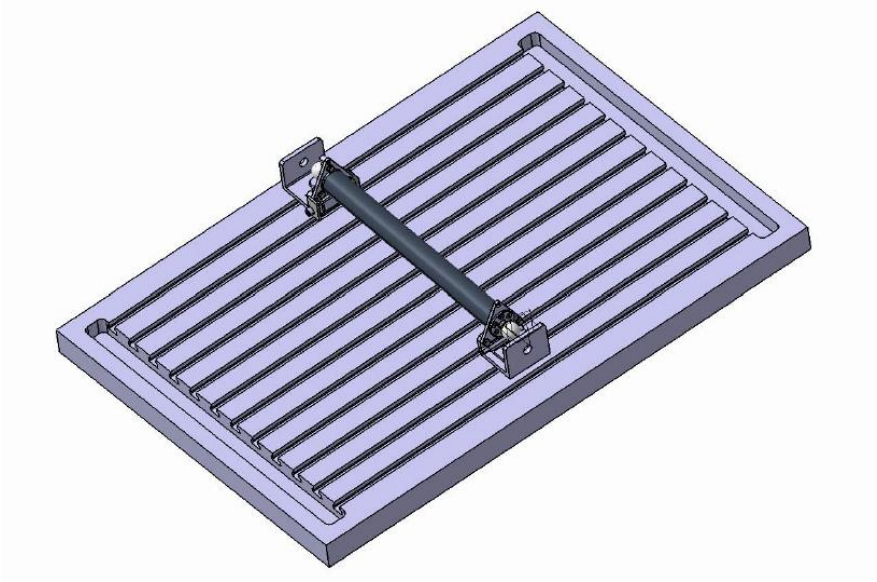

Figure 26: Position of the ball bar in Y-Axis

- For evaluating the "Z" axis scale, the ball standard is mounted with one side to the machine table and with the other side to the tripod, which is also mounted on the machine table. With this combination, the ball standard can be positioned in any direction in the machine working space.

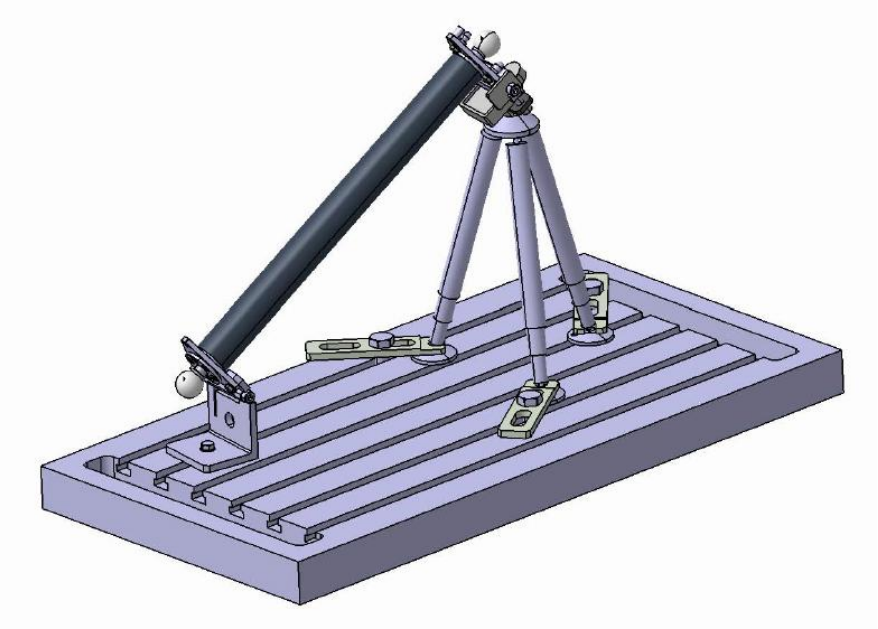

Figure 27: Position of the ball bar in space diagonal

5.7.3 Measurement

The measurand is the distance between ball centres of the ball standard. Measurement is performed by probing eight points on the ceramic balls and by evaluating their centre point coordinates. Four points are probed by a 3D touch probe on each ceramic ball and the ball centre coordinates are evaluated. After that, the distance between ball centres is calculated. Measurement is repeated 15 times in each ball bar position in order to evaluate repeatability s_M, which is included in the uncertainty of measurement (equation on page 34).

Figure 28: Measurement of the ball standard

5.8 Testing procedure – 5 axis milling centre (with tilt/turning table)

5.8.1 Choosing the right standard

Proper length of the ball bar is selected in accordance with Table 2.

5.8.2 Positioning the standard

Standard shall be mounted on the machine working table according to Figure 29, Figure 30, and Figure 31. Measurements are performed in two extreme positions in each axis.

- For evaluating “X” axis scale, the ball standard is set horizontally and placed parallel to x axis. It is mounted by using special clamping elements shown in Figure 20.

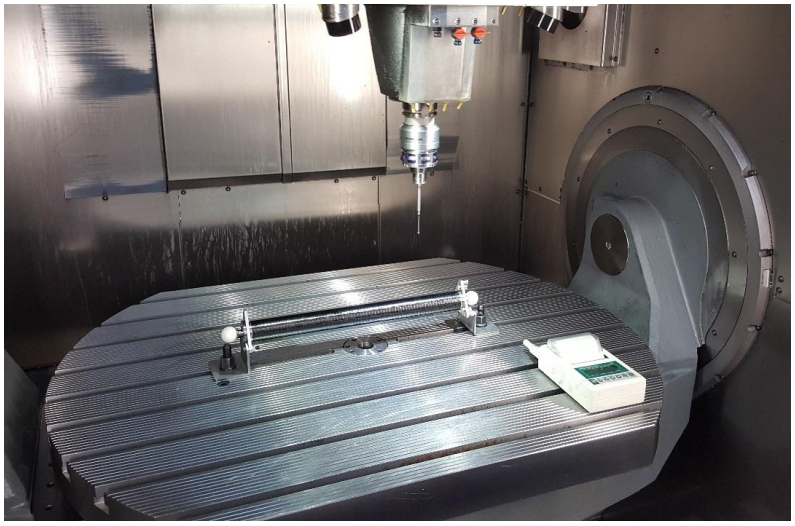

Figure 29: Position of the ball bar in X-Axis

- For evaluating “Y" axis scale, it is not necessary to unmount the ball standard, the working table can be rotated by 90°.

Figure 30: Position of the ball bar in Y-Axis

- For evaluating the for "Z" axis scale, it is not necessary to unmount the ball standard to test the Z axis, the working table can be tilted in both direction by 45° or 90°. (Possible combination is also with the rotation of working table in both directions).

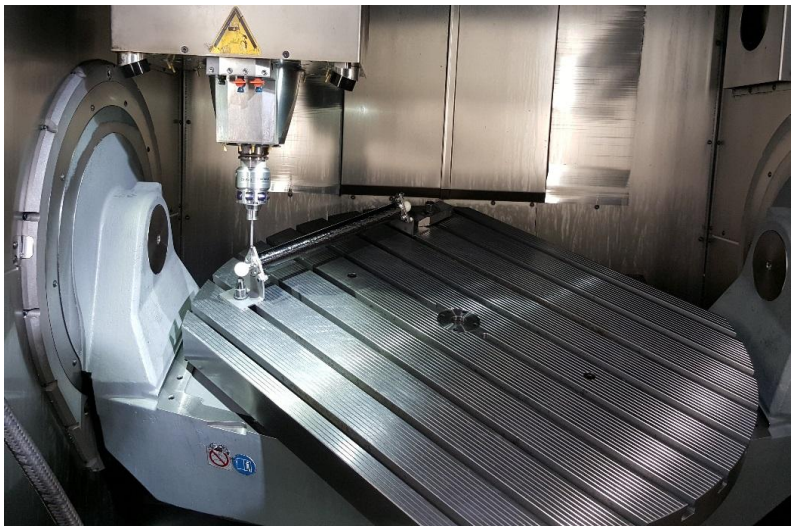

Figure 31: Position of the ball bar in a space diagonal

5.8.3 Measurement

The measurements are performed in the same way as described in 5.7.3 The distance between ball centres is calculated by using the measuring programme on the CNC machine (in case the machine is equipped with such SW).

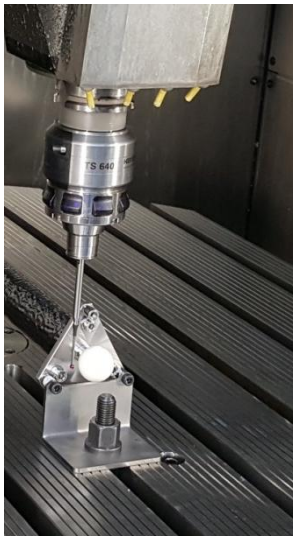

Figure 32: Measurement of the ball standard

5.9 Evaluation of measurement results

Measurement results (calculated distances between ball centres) are compared with calibrated ball bar lengths. Sample presentation of measurement results is shown in Figure 33 and Figure 34. In addition, repeatability is calculated as experimental standard deviation from 15 measurements in a single ball bar position.

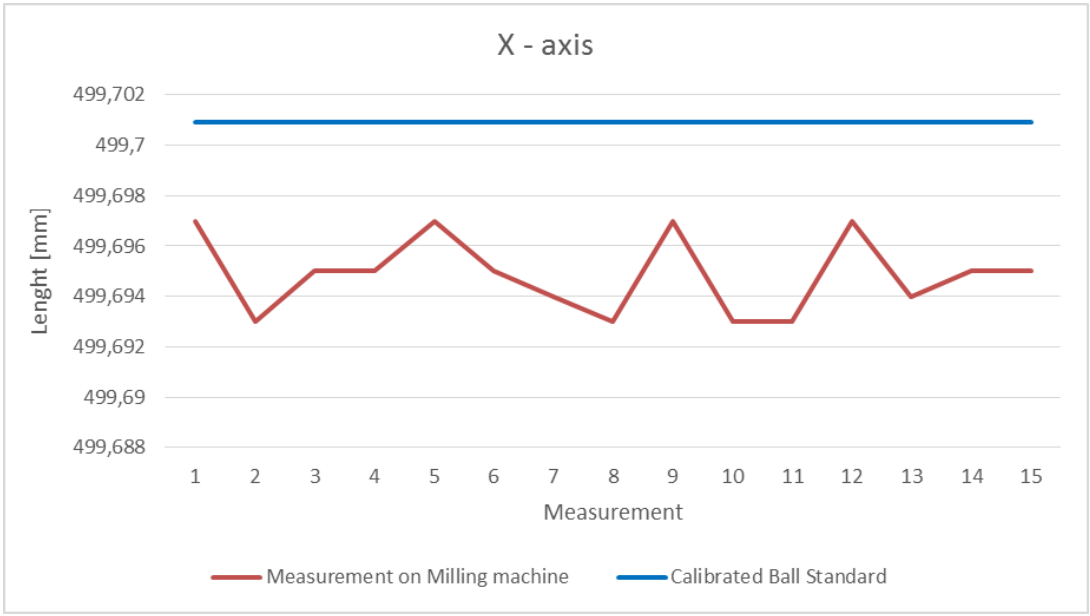

Figure 33: Sample presentation of measured ball bar lengths (15 repetitions)

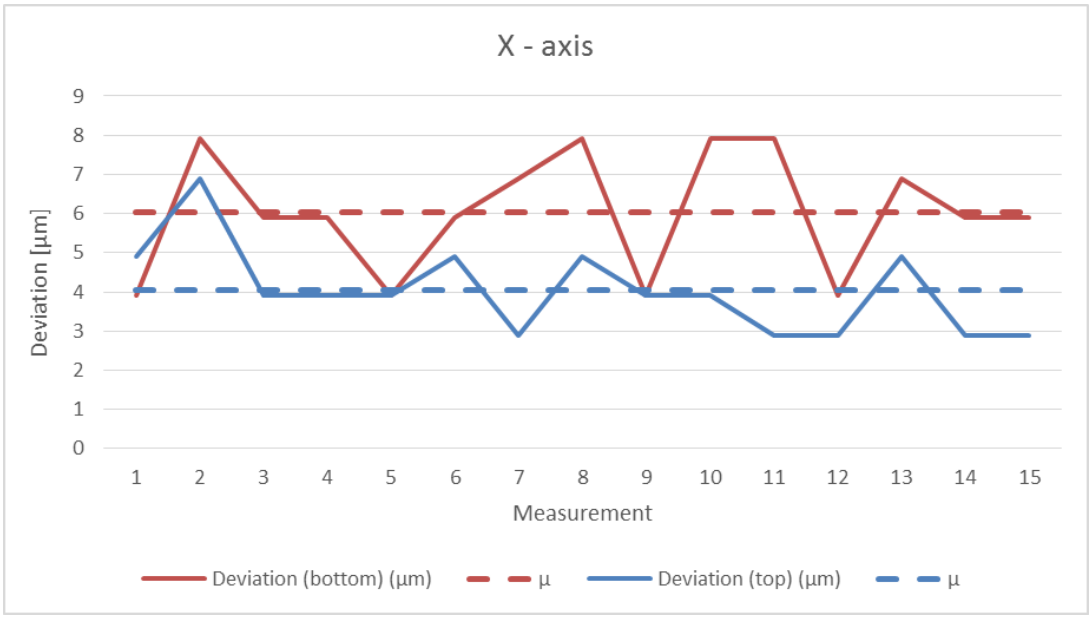

Figure 34: Sample presentation of measured length deviations and mean deviations in one axis (15 repetitions)

The results are compared with machine tool specifications. Based on this information, the machine tool user makes a decision about conformity. The acceptance condition is defined by the following equation:

$$(D \pm U) < MPE$$

where:

- D - measured mean length deviation
- U - expanded test uncertainty (see 5.10)
- MPE - maximum permissible error of the machine tool (specifications)

5.10 Uncertainty of measurement

Total standard uncertainty comprises three main contributions:

- u_p - standard uncertainty of the verification procedure (including uncertainty of the ball bar calibration)
- s_M - standard deviation from 15 repeated measurement (repeatability contribution)
- $u(R)$ - contribution of the resolution of the machine tool measurement system

Standard uncertainty of the procedure was evaluated to be:

$$u_p = 2{,}2\ \mu\text{m} + 4{\cdot}10^{-6}{\cdot}L \quad \text{where } L \text{ is the length of the ball standard}$$

Combined standard uncertainty is calculated after the measurements with the following equation:

$$u = \sqrt{(2{,}2\ \mu\text{m})^2 + {s_M}^2 + R^2/3} + 4{\cdot}10^{-6}{\cdot}L$$

where:

- s_M - standard deviation from 15 repeated measurement
- R - resolution of the machine tool measurement system
- L - length of the ball standard

Expanded uncertainty is:

$$U = 2{\cdot}u \text{ ; level of confidence} \approx 95\ \%$$

6 References

[1] ISO 230-1:2012, *Test code for machine tools - Part 1: Geometric accuracy of machines operating under no-load or quasi-static conditions,* Beuth Verlag, 2012

[2] ISO 230-6:2012, *Test code for machine tools - Part 6: Determination of positioning accuracy on body and face diagonals (Diagonal displacement tests),* Beuth Verlag, 2012

[3] D. Berger, D. Brabandt, G. Lanza, “Conception of a mobile climate simulation chamber for the investigation of the influences of harsh shop floor conditions on in-process measurement systems in machine tools”, *Measurement*, *Vol. 74, pp. 233-237*, Oct. 2015.

[4] H. Schwenke, M. Franke, J. Hannaford, H. Kunzmann, “Error mapping of CMMs and machine tools by a single tracking interferometer”, CIRP Annals - Manufacturing Technology, Volume 54, Issue 1, 2005, Pages 475-478

[5] H. Schwenke, R. Schmitt, P. Jatzkowski, C. Warmann, “On-the-fly calibration of linear and rotary axes of machine tools and CMMs using a tracking interferometer”, CIRP Annals - Manufacturing Technology, Volume 58, Issue 1, 2009, Pages 477-480